Functional and structural insights into Sarcolipin, a regulator of the Sarco-endoplasmic reticulum Ca2+-ATPases

Thomas Barbot, Cédric Montigny, Paulette Decottignies, Marc Le Maire, Christine Jaxel, Nadège Jamin, Veronica Beswick

Chapter 10
Functional and Structural Insights into Sarcolipin, a Regulator of the Sarco-Endoplasmic Reticulum Ca^{2+}-ATPases

Thomas Barbot, Cédric Montigny, Paulette Decottignies, Marc le Maire, Christine Jaxel, Nadège Jamin, and Veronica Beswick

Abstract Sarcolipin (SLN), a transmembrane peptide from sarcoplasmic reticulum, is one of the major proteins involved in the muscle contraction/relaxation process. A number of enzymological studies have underlined its regulatory role in connection with the SERCA1a activity. Indeed, SLN folds as a unique transmembrane helix and binds to SERCA1a in a groove close to transmembrane helices M2, M6, and M9, as proposed initially by cross-linking experiments and recently detailed in the 3D structures of the SLN–Ca^{2+}-ATPase complex. In addition, association of SLN with SERCAs may depend on its phosphorylation. SLN possesses a peculiar C-terminus (RSYQY) critical for the regulation of the ATPases. This luminal tail appears to be essential for addressing SLN to the ER membrane. Moreover, we recently demonstrated that some SLN isoforms are acylated on cysteine 9, a feature which remained unnoticed so far even in the recent crystal structures of the SLN–SERCA1a complex. The removal of the fatty acid chain was shown to increase the activity of the membrane-embedded Ca^{2+}-ATPase by about 20 %. The exact functional and structural

T. Barbot • C. Montigny • M. le Maire • C. Jaxel • N. Jamin
Institute for Integrative Biology of the Cell (I2BC), Commissariat à l'Energie Atomique et aux Energies Alternatives (CEA), Centre National de la Recherche Scientifique (CNRS), Université Paris-Sud, iBiTec-S/SB2SM/Laboratoire des Protéines et Systèmes Membranaires, CEA-Saclay, 91191 Gif-sur-Yvette CEDEX, France

P. Decottignies
Pharmacologie et biochimie de la synapse, Neuro PSI, UMR9197, CNRS, Université Paris-Sud, 91405 Orsay CEDEX, France

V. Beswick (✉)
Institute for Integrative Biology of the Cell (I2BC), Commissariat à l'Energie Atomique et aux Energies Alternatives (CEA), Centre National de la Recherche Scientifique (CNRS), Université Paris-Sud, iBiTec-S/SB2SM/Laboratoire des Protéines et Systèmes Membranaires, CEA-Saclay, 91191 Gif-sur-Yvette CEDEX, France

Physics Department, Université d'Evry-Val-d'Essonne, 91025 Evry CEDEX, France
e-mail: veronica.beswick@cea.fr

S. Chakraborti, N.S. Dhalla (eds.), *Regulation of Ca^{2+}-ATPases,V-ATPases and F-ATPases*, Advances in Biochemistry in Health and Disease 14,
DOI 10.1007/978-3-319-24780-9_10

role of this post-translational modification is presently unknown. Recent data are in favor of a key regulator role of SLN in muscle-based thermogenesis in mammals. The possible link of SLN to heat production could occur through an uncoupling of the SERCA1a-mediated ATP hydrolysis from calcium transport. Considering those particular features and the fact that SLN is not expressed at the same level in different tissues, the role of SLN and its exact mechanism of regulation remain sources of interrogation.

Keywords Sarcolipin • Calcium ATPase • NMR • X-Ray crystallography • Molecular dynamics • Phosphorylation • Protein acylation • Oligomerization • Regulatory peptides • Membrane protein

Abbreviations

SRER	Sarco-endoplasmic reticulumEndoplasmic reticulum
ER	Endoplasmic reticulum
SERCA1a or 2a	Sarco-Endoplasmic Reticulum Ca^{2+}-ATPase isoform 1a or 2a
SLN	Sarcolipin
hSLN	Human isoform of SLN
rSLN	Rabbit isoform of SLN
mSLN	Mouse isoform of SLN
PLN	Phospholamban
DDM	*n*-Dodecyl-β-D-maltopyranoside
$C_{12}E_8$	Octaethylene glycol monododecyl ether
DOC	Deoxycholate
SDS	Sodium dodecyl sulfate
DPC	*n*-Dodecylphosphocholine or Fos-choline-12
SEC	Size exclusion chromatography
MS	Mass spectrometry
MALDI-TOF	Matrix-assisted laser desorption ionization—time of flight
NMR	Nuclear magnetic resonance
ssNMR	Solid state nuclear magnetic resonance
MD	Molecular dynamics
POPC	1-Palmitoyl-2-oleoyl-sn-glycero-3-phosphocholine
DOPC	1,2-Dioleoyl-sn-glycero-3-phosphocholine
DOPE	1,2-Dioleoyl-sn-glycero-3-phosphoethanolamine
EYPC	Egg yolk phosphatidylcholine
EYPA	Egg yolk phosphatic acid
RyR	Ryanodine Receptor
FCCP	Carbonyl cyanide-p-trifluoromethoxyphenylhydrazone

1 Introduction

Sarcolipin is a transmembrane peptide (SLN, 31 amino acids) [1] which was first isolated from rabbit fast-twitch skeletal muscle during the extraction of sarco-endoplasmic reticulum (SR) membranes [2]. Purification and solubility analysis of SLN revealed strong interactions with lipids and the presence of fatty acids. Therefore, considering its amino acid sequence similarity with phospholamban (PLN), a Ca^{2+}-ATPase regulatory peptide, it was suggested that SLN interacts both with lipids and the sarco-endoplasmic reticulum Ca^{2+}-ATPase (SERCA1a) [3, 4].

The main role of SERCAs is to control cytosolic calcium by maintaining SR/ER calcium stores in cells. Calcium is the primary regulator of the contractile machinery and a second messenger in the signal transduction pathways that control, e.g. muscle growth, metabolism, and pathological remodeling. Upon muscle stimulation, Ca^{2+} release by the ryanodine receptor (RyR) localized at the SR membrane transiently increases Ca^{2+} level in the cytosol, triggering actomyosin cross-bridge formation within the sarcomere to generate contractile force. Re-uptake of Ca^{2+} into the SR by SERCAs is necessary for muscle relaxation and restores the Ca^{2+} level for subsequent contraction–relaxation cycles. Several SERCA isoforms have been described with different expression profiles depending on the species, tissues, and even the developmental stage. SERCA1a and SERCA2a isoforms are predominant, and are mainly expressed in the fast-twitch muscle and in the slow-twitch muscle, respectively [5] (Table 10.1 and references herein).

The main steps of the calcium transport cycle are well understood (Fig. 10.1). However, its regulation and especially, the exact role of sarcolipin are still a matter of debate as reviewed below. As a matter of fact, SLN is one of known regulators of SERCA activity in vertebrates as well as phospholamban (PLN, 52 amino acids; [6]) and most probably myoregulin (MLN, 46 amino acids; [7]) (Fig. 10.2). Contrary to SLN and MLN, PLN has been extensively characterized during the last two decades. In invertebrate, an ortholog of these proteins has also been discovered recently and is named sarcolamban (SCL, 28 amino acids; [7, 8]).

In order to contribute to a better understanding of the specific regulator role of SLN upon SERCA activities, we propose, in this review, some critical readings of the published data as well as some additional data. First, SLN gene characterization, its localization in species and tissues and its differential expression during muscle development are presented. Secondly, SLN implications in diseases and thermogenesis are discussed. Then, structural and functional data, including the role of particular amino acid sequence features (phosphorylation, luminal tail, acylation) are reviewed to give a general and new outlook on the topic. Finally, the hypothesis of SLN oligomer formation and SLN interaction with PLN are considered.

Table 10.1 Expression of SLN, PLN, MLN, SERCA1a and SERCA2a in various species and tissues

		Levels of expression (mRNA and proteins) of peptides and SERCA								
		SLN		PLN		MLN	SERCA1a		SERCA2a	
Species	Tissues	mRNA	Proteins	mRNA	Proteins	mRNA	mRNA	Proteins	mRNA	Proteins
Mouse	Atria	$++^{a}$ $+++^{e}$	$+++^{b}$	$++^{a}+++^{e}$	$+/-^{b}$	$-^{e}$	$-^{a}$		$+++^{a}$ $+++^{e}$	$+++^{b}$
	Ventricle	$-^{a}$ $-^{e}$	$-^{b}$	$+++^{a}$ $+++^{e}$	$+++^{b}$	$-^{e}$	$-^{a}$		$+++^{a}$ $++^{e}$	$+++^{b}$
	Slow-twitch muscle	$+^{a}$	$+/-^{b}$	$+/-^{a}$ $-^{e}$	$+/-^{b}$	$+^{e}$	$++^{a}$	$+^{b}$	$++^{a}$ $+^{e}$	$++^{b}$
	Fast-twitch muscle	$-^{a}$	$++^{b}$	$+/-^{a}$ $-^{e}$	$+/-^{b}$	$+++^{e}$	$+++^{a}$	$++^{b}$	$+/-^{a}$ $-^{e}$	$+^{b}$
Rat	Atria	$++^{a}$	$+++^{b}$	$++^{a}$	$+^{b}$		$-^{a}$		$+++^{a}$	$+++^{b}$
	Ventricle	$-^{a}$	$-^{b}$	$+++^{a}$	$+++^{b}$		$-^{a}$		$+++^{a}$	$+++^{b}$
	Slow-twitch muscle	$+/-^{a}$	$+/-^{b}$	$-^{a}$	$-^{b}$		$+^{a}$		$++^{a}$	$++^{b}$
	Fast-twitch muscle	$-^{a}$	$++^{b}$	$-^{a}$	$-^{b}$		$+++^{a}$		$+/-^{a}$	$+^{b}$
Rabbit	Atria	$++^{a}$	$+/-^{b}$	$++^{a}$	$+^{b}$		$-^{a}$		$+++^{a}$	$+++^{b}$
	Ventricle	$-^{a}$	$-^{b}$	$+++^{a}$	$+++^{b}$		$-^{a}$		$+++^{a}$	$+++^{b}$
	Slow-twitch muscle	$++^{a}$	$++^{b}$	$+^{a}$	$-^{b}$		$++^{a}$		$++^{a}$	$+^{b}$
	Fast-twitch muscle	$+++^{a}$	$+++^{b}$	$+/-^{a}$	$-^{b}$		$++^{a}$		$+^{a}$	$+^{b}$
Pig	Atria	$+^{a}$		$+^{a}$			$-^{a}$		$+++^{a}$	
	Ventricle	$+/-^{a}$		$+^{a}$			$-^{a}$		$+++^{a}$	
	Slow-twitch muscle	$+++^{a}$		$+/-^{a}$			$+^{a}$		$++^{a}$	
	Fast-twitch muscle	$+++^{a}$		$+/-^{a}$			$++^{a}$		$++^{a}$	

Dog	Atria		+/−[b]		+/−[b]						+++[b]
	Ventricle		−[b]		+++[b]						+++[b]
	Slow-twitch muscle		++[b]		−[b]						+[b]
	Fast-twitch muscle		+++[b]		−[b]						+[b]
Human	Atria		+++[c]		+++[c]						+++[c]
	Ventricle										
	Slow-twitch muscle		+[d]		+++[d]				+[d]		+++[d]
	Fast-twitch muscle		+++[d]		++[d]				+++[d]		−[d]

Relative evaluations were performed by measuring the mRNA levels (RT PCR) and the proteins levels (western-blots). Selected references are [12][a], [13][b], [16][c], [14][d] and [7][e]

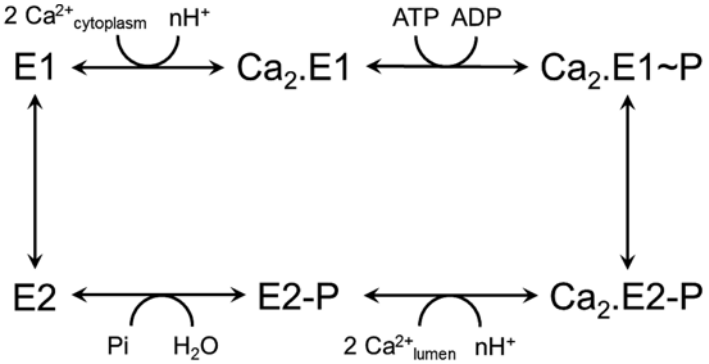

Fig. 10.1 Ca^{2+}-ATPase catalytic cycle. Sarcoplasmic reticulum calcium ATPases catalyze calcium transport from the cytosol to the lumen, coupled with ATP hydrolysis. The main steps of the catalytic cycle are shown here. At physiological pH, two cytoplasmic calcium ions bind to the "E1" high-affinity states. Binding of one Mg.ATP triggers calcium occlusion and it results in autophosphorylation of the ATPase ("Ca_2.E1~P" occluded state). Then, large conformational changes occur, leading to the calcium deocclusion, the release of the calcium into the lumen, and protonation of the transport sites. The Ca^{2+}-free "E2-P" state is finally hydrolyzed to the "E2" ground state

```
hSLN                              MGINTRELFLNFTIVLITVILMWLLVRSYQY
hPLN   MEKVQYLTRSAIRRASTIEMPQQARQKLQNLFINFCLILICLLLICIIVMLL
hMLN        MTGKNWILISTTTPKSLEDEIVGRLLKILFVIFVDLISIIYVVITS
dSCL                              MSEARNLFTTFGILAILLFFLYLIYAVL
                                  *  *  ...  .  .  ..
```

Fig. 10.2 Transmembrane peptides that putatively interact with SERCAs. Alignment of human sarcolipin (hSLN), human phospholamban (hPLN), human myoregulin (hMLN), and their invertebrate ortholog *Drosophila melanogaster* sarcolamban (dSCL). Sequences were aligned with the SEAVIEW program [100]. *Boxed* residues are expected to match with the hydrophobic part of the lipid bilayer. Identical residues are indicated by a *star* and similar residues are *dotted*

2 Sarcolipin Gene Characterization

In human, SLN gene is mapped to chromosome 11q22-q23 [4]. SLN gene (5.6 kb) has two small exons, with the entire coding sequence lying in exon 2 and a large intron (3.9 kb) separating the two segments. Several box elements upstream of the transcription initiation site may correspond to DNA binding sites for transcriptional activators such as (a) the binding site for the myocyte enhancer factor MEF2 in combination with MEF3-like element involved in muscle-specific induction of the aldolase A gene, and (b) the E box-paired sites for MyoD bound in the muscle creatine kinase enhancer [9] and in the acetylcholine receptor α-subunit enhancer [10]. Thus, these DNA binding elements might be responsible for the muscle-specific expression of the SLN gene. The 3′ end of the gene contains multiple polyadenylation signals and two transcripts may be produced, one being preferential.

Comparison of human, rabbit, and mouse SLN cDNAs revealed 84 % nucleotide sequence identity between human and rabbit, 44 % nucleotide sequence identity between human and mouse, and 41 % sequence identity between mouse and rabbit SLN cDNAs. The higher level of nucleotide sequence identity between human and rabbit SLN cDNAs is reflected in their identical length and in their use of the same polyadenylation signal sequence for the major transcript. This polyadenylation site is lacking in the mouse SLN gene, which contains another consensus polyadenylation signal sequence downstream. Thus, the mouse cDNA is longer. In terms of translation, nucleotides including the translation initiation signal sequence [11] are not well conserved among the three species [4].

The two other membrane peptides, PLN and MLN, have a similar gene organization. As a matter of fact, the human PLN gene, as the SLN gene, contains two exons and one large intron (6 kb), the entire coding sequence being located in exon 2. The 3′ end of the PLN gene also contains multiple polyadenylation signals. Recent genome-wide studies have suggested that hundreds of functional peptides may be also encoded in vertebrate long noncoding RNAs (lncRNAs) notably in humans and mice. While analyzing the evolutionary conservation of lncRNA, Anderson et al. recently identified an annotated skeletal muscle-specific lncRNA and a short 138 nucleotides ORF with the potential to encode a highly conserved 46 amino acid peptide, myoregulin (MLN) [7]. The human and mouse MLN genes consist of three exons that span 16.5 kb and 15 kb, respectively, with the ORF located in exon 3. MLN, the skeletal muscle-specific isoforms of SERCA and the Ryanodine receptor (RyR) are co-regulated by MyoD, suggesting that they comprise a core genetic module important for Ca^{2+} handling in skeletal muscle. Analysis of the 5′ flanking region of the MLN gene revealed highly conserved binding sites for the myogenic transcription factors MyoD (E-box) and MEF2. Thus, the MLN gene is a direct target of the transcription factors that activate skeletal myogenesis as the SLN gene [7, 9].

3 Expression of Sarcolipin in Species and Tissues

3.1 Expression of mRNA Encoding Sarcolipin

In order to describe SLN expression at the mRNA level, Odermatt et al. have performed Northern blots analyses by using a human probe against the 3′ untranslated region of the cDNA [4]. Using this method, no expression of SLN was found in various human tissues such as brain, placenta, lung, liver, kidney, uterus, colon, small intestine, bladder, and stomach. Only trace amounts were detected in prostate and pancreas. Yet, the SLN transcript was highly expressed in skeletal muscle at least 50-fold more abundant than in heart muscle. By using a similar rabbit probe, a ninefold higher level of the SLN transcript was found in rabbit fast-twitch skeletal muscle (*psoas*) than in slow-twitch skeletal muscle (*soleus*).

SLN expression at the mRNA level and in various species was more recently determined by RT-PCR experiments. Vangheluwe et al. have shown a difference of

SLN mRNA level in small mammals (mouse and rat) as compared to large mammals (rabbit and pig) [12]. Indeed, SLN mRNA was found in *atria* for rodents, while it was detected in *atria*, *soleus* and *extensor digitorum longus* (EDL) for rabbit, and at very high level in *soleus* and EDL for pig. By comparison, PLN mRNA was detected at very high level in ventricles for rodents and rabbit (at lower level for pig), in *atria* for all the species and also in *soleus* for rabbit. In terms of SERCA1a and SERCA2a mRNA, SERCA2a is the only isoform found in heart (ventricle and *atria*) for all studied species, SERCA2a is more expressed than SERCA1a in *soleus* for all the species, and SERCA1a is largely the major form in EDL for all the species except for pig (where SERCA2a is more abundant than SERCA1a) (see Table 10.1).

The SLN expression was also studied at the protein level. To perform such studies, the authors have generated an antibody targeted to a peptide corresponding to the N-terminal sequence (12 residues) of mouse SLN [12]. This antibody reacts to mouse SLN as expected but the authors noticed that this antibody could also cross-react with PLN and, has a very low affinity for rabbit and pig SLN, probably due to sequence diversity at the N-terminus of SLN between small and larger mammals. Consequently, the use of this antibody was restricted to rodents (see Fig. 10.3a for sequences). Western blot analyses of SLN abundance confirmed the expression of SLN in *atria* for rodents. Using a highly specific antibody, targeting the C-terminal sequence (6 residues) of SLN which is conserved among most of the species (see below), Babu et al. have shown that SLN is more abundant in rodent *atria* (mouse, rat) than in *atria* of larger mammals (rabbit, dog) [13]. In rodents' *atria* and ventricles, the high levels of expression of SLN and SERCA2a are correlated, whereas in rabbit and dog, SLN is predominantly expressed in muscle tissues although SERCA2a expression is moderate (see Table 10.1). Recently, SLN was found in human *vastus lateralis* skeletal muscle only in the presence of SERCA1a and, in fast-twitch muscle fibers while PLN is expressed in fast-twitch and slow-twitch fibers, with a preference for slow-twitch fibers, where SERCA2a is predominant [14] (see Table 10.1).

3.2 Differential Expression of Sarcolipin during Muscle Development

Babu et al. have studied whether SLN expression may be developmentally regulated [13]. The authors analyzed the temporal pattern of SLN expression in rat *atria*, ventricle, quadriceps, and tongue during embryonic and neonatal development. SLN was detected in the *atria* and its expression level increases throughout development, whereas in the ventricle, its expression level was below detection. At the same development stage, PLN was detected only in heart tissues and the expression level was higher in the ventricles. During embryonic development, the fast-twitch muscle undergoes several transitions from slow- to fast-twitch fibers. Thus, in rat fast-twitch skeletal muscles as the quadriceps muscles, SLN and SERCA2a are expressed at

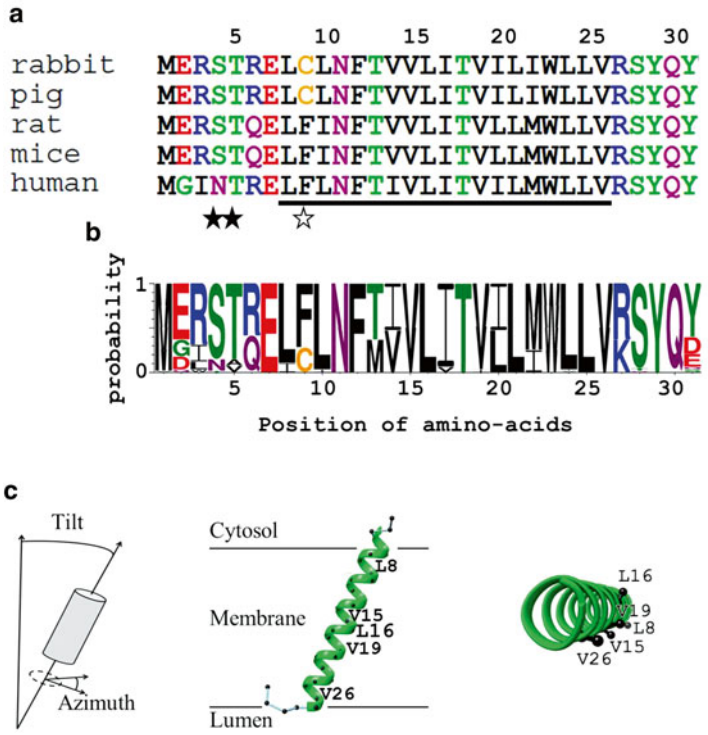

Fig. 10.3 Sarcolipin. (**a**) The alignment of selected sequences was obtained with the SEAVIEW program [100]. Serine 4 and Threonine 5 were identified as putative phosphorylation sites for Ca^{2+}-calmodulin-dependent kinases or STK16 kinases (*black stars,* [32, 33]). In rabbit and pig, cysteine 9 is constitutively acylated (*white star*, [31]). The region of SLN predicted to match with the hydrophobic part of the lipid bilayer is *underlined.* (**b**) A sequence logo [101, 102] was obtained from the alignment of 110 sarcolipin sequences (for detailed procedure, see [31]). Color code for panels **a** and **b** is the following: acidic residues in *red*, basic residues in *blue*, cysteine in *yellow*, Q and N in *pink*, other polar residues and glycine in *green*, and *black* for hydrophobic residues. The *height of the letters* corresponds to the relative frequency of each amino acid at a given position. (**c**) *left*, definition of the tilt and azimuthal angles; *middle*, hSLN helical structure and its orientation within the bilayer, with the N-terminus pointing in the cytosol and the C-terminus pointing in the lumen; *right*, hSLN helix viewed from the luminal side of the membrane [39]. Only the residues of the helix side oriented toward the lumen are depicted. For the sake of clarity, only α and β carbons are represented by *small black spheres* on *right panel*

high levels throughout embryonic development. After birth, SLN and SERCA2a protein levels decline and disappear after 21 days. In contrast, SERCA1a expression increases and SERCA1a becomes the predominant SERCA isoform in the adult. In parallel, during mouse embryogenesis, MLN might be expressed in the precursors of skeletal muscle as estimated from the mRNA levels (using northern-blot analysis with a probe specific to the full-length MLN transcript). During fœtal and adult stages, MLN mRNA is found in all skeletal muscles, similarly to the expression pattern of SERCA1a, and is not detected in cardiac or smooth muscles [7].

4 Sarcolipin in Health and Diseases

As human SLN is highly expressed in *atria* and mediates β-adrenergic responses, its involvement in various heart diseases has been investigated. Both at mRNA and protein levels, SLN expression has been shown to be altered in the atrial myocardium disease [15] so SLN is proposed to be a key regulator of cardiac SERCAs. SLN mRNA levels are decreased in *atria* of patients with chronic atrial fibrillation (AF). SLN protein expression level is also significantly decreased both in patients with atrial fibrillation (AF) and in those with heart failure (HF). Although PLN protein level is not altered, PLN phosphorylation is significantly decreased in the atrial tissues of patients with AF and HF compared to control patients. The Ca^{2+} sensitivity as well as the V_{max} of SR Ca^{2+} uptake is significantly increased in human *atria* from AF patients [16]. In children with congenital heart defects (tetralogy of Fallot), at the mRNA level, SLN and PLN expressions were decreased relatively to SERCA2a and RyR2 expressions [17].

In large mammals and human, SLN is also highly expressed in fast-twitch muscle fibers associated with SERCA1a. Thus, diseases related to muscle dysfunctions have been studied. The Brody disease is an inherited disorder of skeletal muscle function characterized by exercise-induced impairment of muscle relaxation. Studies of the sarcoplasmic reticulum from Brody patients have shown a decrease of the Ca^{2+} uptake and the Ca^{2+}-dependent ATP hydrolysis. As a matter of fact, SERCA1a activity was reduced by 50 % even if the SERCA1a content was reported to be normal in all patients. Mutations in the *ATP2A1* gene encoding SERCA1a have been associated with the Brody disease in some families (called Brody disease with *ATP2A1* mutations), but not in other families (called Brody syndrome without *ATP2A1* mutations) [18]. As SLN interacts with SERCA1a, it was proposed that SLN gene could be altered in Brody disease, because a mutation of SLN could increase inhibition of SERCA1a function. However, no alteration in coding, splice junctions or promoter sequences was found in the SLN gene [4].

The SERCAs and more recently SLN have been proposed to play a key role in non-shivering thermogenesis (reviewed in [19, 20]). Animals lacking brown adipose tissues produce heat from ATP hydrolysis to maintain their body temperature [19, 21]. Moreover, regulation of thermogenesis is critical for cold acclimation [19]. There are functional similarities in the use of the skeletal muscle for thermogenesis across several animals, like fishes, birds, and mammals [19]. De Meis et al. suggested that part of the energy released from the hydrolysis of ATP at the SR, i.e. by the Ca^{2+}-ATPase, could be dissipated as heat, while the other part of the energy would be used to drive the transport of calcium ions through the membrane [22]. As suggested by de Meis et al. this process could involve the release of calcium from the $Ca_2.E_2$-P state in the cytosol instead of in the lumen, yielding a futile hydrolysis of ATP since all the energy would be dissipated as heat. This phenomenon was named slippage or uncoupling [23–25]. Interestingly, the rate of slippage is affected by the presence of sarcolipin. SLN when co-reconstituted with SERCA1a, increases the rate of uncoupling, resulting in an increase of the heat production whereas the

accumulation of calcium decreases [20]. Using isothermal calorimetry, it was shown that the amount of heat production is maximal at a SLN:SERCA1a 15:1 mol:mol ratio [26]. As reported in Table 10.1, the SLN content of SR depends on the muscle type. Therefore, SLN expression level could vary with the involvement of a given muscle in thermogenesis. This hypothesis gave rise to several studies in order to demonstrate the specific in vivo role of SLN in thermogenesis [27]. Recently, SLN was shown to have a protective role against hypothermia and obesity induced by high fat diet using a knock-out mouse model [28, 29]. As a matter of fact, it is suggested that this protective role results from an increase in the uncoupling of the SERCA1a, but also that the ryanodine receptor 1 Ca^{2+} channel may play a role in thermogenesis [28, 30].

5 Structure of Sarcolipin

5.1 Primary Structure

Sarcolipin possesses 31 residues and is composed of three regions (Fig. 10.3a). For most of the species, the N-terminus (1–7) is rich in polar and charged residues as illustrated by Fig. 10.3b. For some species ([31], see also Fig. 10.3b), several charged residues are replaced by neutral or hydrophobic residues, for example ^{1}MERST for rabbit is replaced by ^{1}MGINT for human. The N-terminus, oriented toward the cytosol [3], contains potential phosphorylation sites (Ser4 and Thr5) [32, 33]. On the contrary to the N-terminus, the C-terminus amino acid sequence, ^{27}RSYQY, is highly conserved. The central region, from Leu8 to Val26, is mainly composed of hydrophobic residues and possesses, in some species, a cysteine at position 9 that was recently shown to be acylated ([31], see below).

5.2 3D Structure of Isolated Human Sarcolipin

Human sarcolipin structure, at atomic resolution, has been extensively studied by solution and solid-state NMR spectroscopies. Solution NMR spectroscopy is performed on membrane proteins solubilized in detergent micelles. This technique is limited to small membrane proteins due to the large size of protein-detergent complexes and to the internal dynamics of membrane protein within the complex. NMR data yield spatial information, such as range of distances between atoms, which is then applied as experimental constraint during molecular modeling. A set of 3D structures compatible with the NMR data is finally obtained. Solid-state NMR (ssNMR) allows the study of membrane proteins in lipid environments such as lipid vesicles or oriented bilayer systems. ssNMR provides information on the secondary structure adopted by the protein and on the orientation of the helices inside the

bilayer (tilt angle of the helix relative to the direction of the magnetic field and the rotation angle around the helix axis, i.e. azimuthal angle, Fig. 10.3c). It can also give high-resolution information on the side-chain conformations [34, 35].

The solution and ssNMR experiments performed on hSLN solubilized in SDS [36] or DPC [37, 38] micelles as well as embedded in DOPC/DOPE bilayers [39] have revealed that hSLN folds as a unique transmembrane helix. The protein adopts a helical structure from residue Glu7 to Arg27 when solubilized in DPC micelles but extends up to residue Ile3 when embedded in a lipid bilayer. This later result is in agreement with results from molecular dynamics (MD) simulations performed on hSLN inserted in a pure DOPC bilayer [40]. It is noteworthy that the sole structure of human SLN found in the PDB (PDB ID: 1jdm) comes from the oldest data obtained by solution NMR experiments performed on hSLN solubilized in the presence of SDS and are consistent with a shorter α-helix structure defined from residue Phe9 to residue Arg27 [36]. The somewhat shorter helical structure observed in the presence of SDS demonstrates the influence of the nature of the detergent headgroup, used to solubilize the protein, on the structure of the N-terminus of hSLN. The transmembrane domain of hSLN solubilized in the presence of DPC encompasses a flexible helix up to residue Ile14 and a more rigid ideal alpha-helix from residue Val15 to residue Arg27 [37, 38]. MD simulation of hSLN in DOPC bilayer confirms the presence of these two different helical flexible regions, responsible for a curved structure [40]. However, Veglia and co-workers have recently proposed that hSLN adopts a helical conformation closer to an ideal helix for the whole sequence from Ile3 to Arg27 when applying solid-state NMR experimental restrained in their simulations [41]. Besides, ssNMR showed that hSLN helix is tilted with respect to the membrane normal. In DOPC/DOPE lipid mixture, the tilt angle is 23 ± 2° [39, 42] in good agreement with the value derived from MD simulations of hSLN in DOPC bilayers which is 28 ± 6° [40] and also with the value obtained by solid-state NMR of hSLN in pure DOPC bilayer [43]. Moreover, experiments and MD simulations have revealed that the residues Leu8, Val15, Leu16, Val19, and Val26 located on the same side of the tilted helix point toward the lumen [39, 40] (Fig. 10.3c). This tilt and this azimuthal position of the helix are driven by the N- and C-terminal residues which undergo specific interactions with the lipid membrane at the water/lipid interfaces. As a matter of fact, MD simulation showed that the N-terminal residues Met1 and Ile3 are located outside the cytosolic interface, the polar residue Thr5, a putative phosphorylation site of SLN [32, 33], interacts with the lipid headgroups as well as Arg6 which forms a salt bridge with the lipid headgroups. On the luminal interface, both C-terminal residues Tyr 29 and Tyr31 interact with lipids via cation–π interactions between the aromatic rings and the lipid choline groups. Arg27 also forms a salt bridge with the lipid headgroups. Moreover, as expected, hydrophobic amino acids are located within the hydrophobic core of the membrane bilayer. The two hydrophilic residues, Thr13 and Thr18, distributed in the center of the lipid bilayer, have their polar hydroxyl groups hydrogen bonded with the backbone carbonyl groups of Phe9 and Ile14, respectively [40].

6 SLN Affects Moderately the Affinity for Ca^{2+} and the V_{max} of SERCA

The possible role of sarcolipin on SERCA isoforms turnover was investigated in various experimental models. One widespread model since the discovery of sarcolipin involves the heterologous expression of SLN and SERCA isoforms in HEK-293 cells [3]. Cells are simultaneously transfected with several genes coding regulatory peptides like SLN or PLN and a SERCA isoform (SERCA1a or 2a). These cell lines, derived from Human Embryonic Kidney cells (HEK cells) [44] do not appear to express endogenously SLN, PLN, SERCA1a and SERCA2a, and are thus good models to assess the role of SLN on SERCA isoforms. Nevertheless, the presence of partners playing a regulatory role is unknown (e.g. RyR, kinases). The coding sequences were inserted in a pMT2 expression vector, under the control of a SV40 strong constitutive promoter, one obvious drawback is the uncontrolled expression level of the different proteins. This lack of control of the protein expression levels of each partner could explain some discrepancies within the published results. MacLennan et al. first showed that co-expression of rabbit SLN with rabbit SERCA1a in HEK-293 cells results in a moderate decrease in the affinity for calcium ($Ca_{1/2}$ rises from 0.3 to 0.5 µM in absence or in presence of sarcolipin, respectively) combined with a huge increase in the V_{max} of about 40 % at micromolar, i.e. saturating, concentrations of calcium [3]. Surprisingly, the same group showed some years later that co-expression in HEK-293 cells of SERCA1a or SERCA2a in presence of SLN resulted in a slight decrease of about 5–10 % of the V_{max} which is far from the initial results [45–47]. However, the authors confirmed that the presence of SLN induces a moderate but reliable decrease in $Ca_{1/2}$ for the two isoforms (0.20 and 0.33 µM for SERCA1a, and 0.13 and 0.37 µM for SERCA2a, in the absence and in the presence of SLN, respectively) [45–47]. As mentioned, the stoichiometry is not tightly controlled during co-expression and this could explain the discrepancies of the results obtained for such heterologous expression systems.

Interestingly, Hughes et al. studied the stoichiometry of the interaction between sarcolipin and SERCA isoforms using rabbit SERCA1a prepared from native sarco-endoplasmic reticulum membranes and a synthetic rabbit SLN co-reconstituted in DOPC bilayers [43, 48]. The authors demonstrated that a 10:1 (SLN:SERCA1a) molar ratio is necessary to observe a moderate decrease in calcium affinity and in V_{max} ($Ca_{1/2}$ rises from 0.2 to 0.5 µM and V_{max} decreases from 1.5 to 1.2 µmol hydrolyzed ATP.mg^{-1} min^{-1}, in absence or in presence of SLN respectively). A 3:1 molar ratio has no effect on SERCA1a turnover. This observation was confirmed in similar studies using a value of the SLN:SERCA1a molar ratio after co-reconstitution in EYPC/EYPA bilayers of about 1:1 to 4.5:1 [49, 50]. At low molar ratio, no effect on V_{max} was found whereas V_{max} decreased by 20 % at the highest molar ratio. A moderate decrease in calcium affinity ($Ca_{1/2}$ rises from 0.4, in absence of SLN, to 0.8 µM, in presence of SLN) was found. Moreover, the presence of endogenous SLN (or PLN) in the samples must be considered as it could affect the stoichiometry. As a matter of fact, native sarco-endoplasmic reticulum membranes prepared from rabbit

fast-twitch skeletal muscle already contains endogenous sarcolipin that could reach about 1:1 SLN:SERCA1a mol:mol [3]. We recently demonstrated that most of the sarcolipin remains associated with SERCA1a even after treating the membranes with deoxycholate (*DOC-extracted SR*) and also even after membrane solubilization by mild detergent [31]. Size exclusion chromatography purification of the DDM-solubilized SR shows that the SLN is mainly co-eluted with SERCA1a at about a 1:1 mol:mol ratio. Some SLN is also detected in the mixed micelles peak suggesting that in the SR membrane, the SLN to SERCA1a ratio is higher than 1:1 mol:mol [31]. Therefore, it is suggested that the results presented above based on co-reconstitution experiments were obtained in presence of misestimated amount of SLN [49, 50, 43, 48, 31]. For example, the lack of effect observed at low molar ratio (proposed to be 1:1 SLN:SERCA1a) is not surprising as it is probably related to a molar ratio higher than 2:1 considering the endogenous SLN content. This point appears to be critical for the interpretation of mutagenesis experiments as both wild-type and mutated SLN are present [50]. In addition, as reported in Table 10.2, some experiments were performed with SERCA and SLN isoforms from different species and sometimes within the same experiment. But, as mentioned previously, the amino acid sequences of SLN differ among species especially the N-terminus (Fig. 10.3a, b) [14, 3, 12]. For example, human SLN reconstituted in presence of rabbit SERCA1a has a lower inhibitory effect than rabbit SLN [38, 49, 50]. In the case of rabbit SLN overexpressed in presence of rat SERCA1a or SERCA2a in rat

Table 10.2 $Ca_{1/2}$and V_{max} estimates in several selected references

SLN [a]	SERCA [a]	Systems used [b] and SLN:SERCA molar ratio [c]	$Ca_{1/2}$ (μM) [d]		V_{max} [e] (% of SERCA alone)	References
			No SLN	+ SLN		
rSLN	rSERCA1a	HEK-293 cells	0.3	0.5	143	[3]
rSLN	rSERCA1a	HEK-293 cells	0.2	0.33	95	[45, 47]
rSLN	rSERCA2a	HEK-293 cells	0.13	0.37	90	[45, 47]
rSLN	rSERCA1a	DOPC bilayers (10:1)	0.2	0.5	80	[43, 48]
hSLN	DOC-extracted rSERCA1a	EYPC-EYPA bilayers (4.5:1)	0.4	0.6	80	[49]
rSLN	DOC-extracted rSERCA1a	EYPC-EYPA bilayers (4.5:1)	0.4	0.8	70	[50]
hSLN	rSERCA1a	DPC micelles	0.25	0.5	100	[38]
rSLN	rat SERCA1a	Slow-twitch myocytes	0.4	0.4	70	[51]

[a]"r" referred to rabbit isoforms, "h" to human isoform

[b]HEK-293 cells and myocytes were used for co-expression and possible microsomes preparation. DOPC or EYPC-EYPA bilayers were obtained from co-reconstitution of SR from native sources with recombinant or synthetic SLN

[c]Molar ratio does not take into account the possible presence of endogenous SLN

[d]$Ca_{1/2}$ corresponds to the amount of calcium necessary to attain half-maximal activity (calcium uptake or turn-over depending on the system used)

[e]Unfortunately, values of V_{max} in $\mu mol.mg^{-1}.min^{-1}$ were not available

myocytes (which are deprived in endogenous SLN) no effect on affinity was detected but a significant decrease of about 30 % in calcium uptake and a reduced contractility were observed [51].

To put it in a nutshell, stoichiometry appears to be one of the critical points to assess diligently the effect of SLN on the SERCA1a catalysis. Neither heterologous expression nor co-reconstitution experiments described here gave an accurate estimate of the SLN:SERCA ratio while yet they all agreed that this ratio is important. Nonetheless, it is widely accepted that sarcolipin is an inhibitor of SERCAs but the detailed mechanism of this inhibition remains unknown at the molecular level.

7 Structural Insights into the SLN–SERCA1a Complex from NMR and X-Ray Diffraction Experiments

7.1 NMR Studies of the Interaction between hSLN and SERCA1a

Studies of the hSLN–SERCA1a interactions were performed using solution NMR spectroscopy of hSLN upon addition of SERCA1a in the presence of DPC. Analysis of both chemical shifts and peak intensities of SLN signals indicate the existence of three different SLN states: the free, the bound, and the intermediate states at the NMR time scale. The effects of the binding were inferred by analyzing the changes occurring in the intermediate form as the bound state of SLN cannot be detected due to the large size of the SLN/SERCA1a/DPC complex.

Changes in ^{1}H chemical shifts were used as reporters for structural changes occurring in hSLN upon interaction with SERCA1a. As a matter of fact, these changes are correlated with variations in hydrogen bond interactions or secondary structures upon interaction [52]. The different flexible regions of isolated hSLN previously identified have distinct properties in the presence of SERCA1a. Concerning the N-terminus, residues Met1 through Arg6, except Asn4, do not exhibit significant chemical shift changes indicating that this region remains highly dynamic in the presence of SERCA1a. In contrast, signals from the helical region spanning residues Glu7 through Val26, which contains two dynamical domains, show large chemical shift changes. Signals from Glu7 to Thr18 (except Thr13) display downfield shifts, whereas signals from the C-terminal portion of the transmembrane helix exhibit an increasing upfield shift for all the residues up to Val26. Buffy et al. have suggested that these chemical shift changes could indicate the formation of tighter hydrogen bonds in the region from Glu7 to Val14 and a slight unwinding of the helix from residues Val15 through Arg27, a mechanism analogous to that proposed for the transmembrane domain of PLN [38]. Concerning the unstructured C-terminal tail, all signals, except those of Arg27, are shifted upfield which could reveal a structural change of this amino acid sequence suggesting an interaction of the tail with either the luminal part of the ATPase or the lipids.

7.2 X-Ray Diffraction of the rSLN–SERCA1a Complex

Two recent crystallographic structures of rabbit SLN in complex with rabbit SERCA1a (PDB ID: 3W5A at a resolution of 3.0 Å [53] and PDB ID: 4H1W at a resolution of 3.1 Å [54]) revealed a previously undescribed conformation of SERCA1a in the presence of SLN. This SERCA1a–rSLN complex was obtained in the presence of high concentration of magnesium (40–75 mM) that appears to be essential to stabilize a Ca^{2+}-deprived form of the enzyme. Considering the relative position of the ATPase sub-domains and the conditions of crystallization, authors from the two groups suggested that this complex corresponds to a genuine E1 intermediate, i.e. between the protonated E2 form and the Ca_2.E1P occluded state (Fig. 10.1). This complex could allow cytoplasmic ion exchange between protons and calcium ions: as a matter of fact, both structures display a large open groove, followed by a deep, funnel-shaped and negatively charged path that leads to the transmembrane Ca^{2+} binding sites, suggesting that this form is prefiguring the Ca^{2+} fixation.

However, the physiological significance of this E1-Mg state is also worth discussion. In both studies mentioned above [53, 54], the structures were solved with the Ca^{2+}-free enzyme solubilized in $C_{12}E_8$, a condition known to cause irreversible enzyme inactivation [55–58]. Besides, the functional role of the E1-Mg state is unclear. On the one hand, Toyoshima et al. concluded that this state is an obligate intermediate in the catalytic cycle of SERCA1a and that Mg^{2+} binding accelerates Ca^{2+} binding by reducing the energy required for formation of a calcium-bound E1 form. On the other hand, Winther et al. concluded differently, that Mg^{2+} binding to the "low-affinity Mg^{2+} sites" actually delays SERCA1a activation by Ca^{2+}. Moreover, Akin et al. [59] concluded that the E1-Mg state obtained at 40–75 mM $MgSO_4$ by Toyoshima et al. and Winther et al. does not exist at a physiological Mg^{2+} concentration (i.e. about 3 mM).

Analyses of both structures [53, 54] reveal that in the complex, rSLN forms a slightly bended membrane-spanning helix, and is associated with SERCA1a within a groove between M2, M6, and M9 transmembrane helices (Fig. 10.4a). Most of the residues located at the interface between rSLN and SERCA1a are hydrophobic amino acids. Those residues form a large hydrophobic cluster (Fig. 10.4b) as represented by the important network of distances less than 4.7 Å between rSLN and SERCA1a hydrophobic side-chains (orange and blue dotted lines). Moreover, rSLN and SERCA1a also show proximities between polar residues. For example, rSLN Asn11 side-chain and SERCA1a Gly801 backbone form a hydrogen bond (Fig. 10.4c), as well as rSLN Glu7 side-chain and SERCA1a Asn111 side-chain (Fig. 10.4d). N-terminal and C-terminal residues of SLN are poorly defined. The local disorder of the electron density maps suggests that no stable interaction involves rSLN C-terminus and SERCA1a in the conditions used for crystallization [54]. These structures are also in agreement with several site-directed mutagenesis experiments: as a matter of fact, MacLennan et al. observed a moderate but significant loss of inhibition after substitution by alanine of SLN Asn11, Val14 and

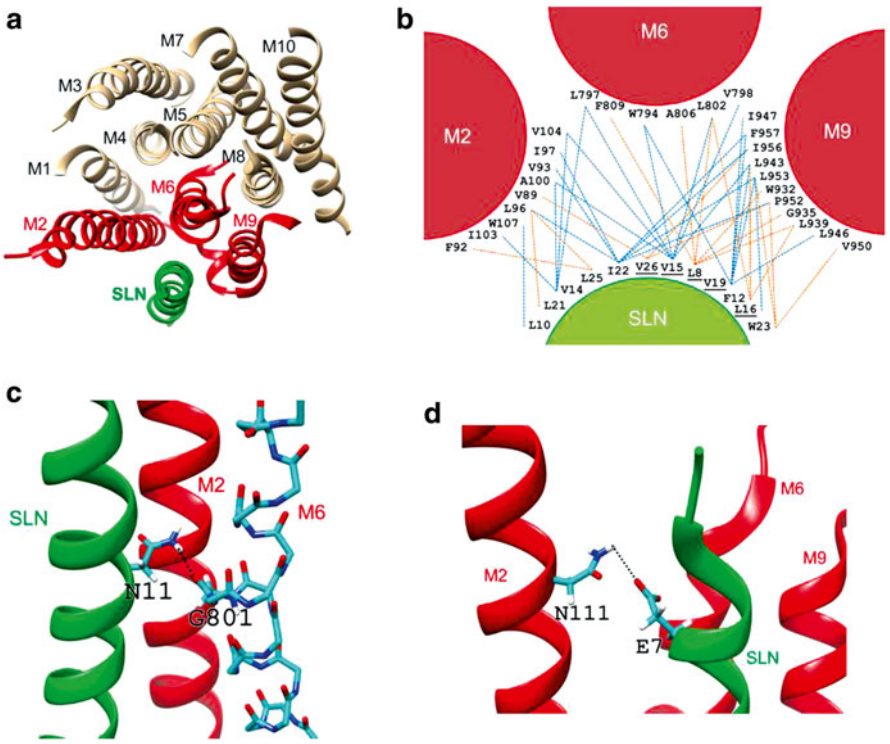

Fig. 10.4 rSLN in interaction with SERCA1a transmembrane domain. (PDB: 4H1W, [54]). (**a**) rSLN is in interaction with SERCA1a within a groove between M2, M6, and M9 transmembrane helices (viewed from the cytosol). Sarcolipin is depicted as a *green ribbon*. SERCA1a transmembrane helices M2, M6, and M9 are depicted as *red ribbons* and the other transmembrane helices are in *grey*. (**b**) Scheme of the hydrophobic interaction network taking place at rSLN/SERCA1a interface (viewed from the cytosol). Only the hydrophobic amino acids involved in the interaction network are displayed. SLN residues previously pinpointed in Fig. 10.3c are underlined. A distance of 4.7 Å or less between side-chains is represented by *blue* or *orange dotted lines* for a sake of clarity. (**c**) rSLN Asn11 side-chain and SERCA1a Gly801 backbone form a hydrogen bond [54]. (**d**) rSLN Glu7 side-chain and SERCA1a Asn111 side-chain form a hydrogen bond [53]. Residues backbone and side-chains are represented as *sticks*. Carbon atoms are in cyan, oxygen in *red*, nitrogen in *blue*, and hydrogen in *white*. Hydrogen bond is represented as a *dotted black line*

Val19 [3]. These authors also showed that substitution by alanine of SERCA1a Leu321 (M4) and Leu802 (M6) trigger SLN dissociation [46]. Additional cross-linking experiments confirmed that the binding sites of SLN and PLN overlap as expected, due to similarities between the SLN transmembrane domain (from Leu8 to Val26) and the membrane-spanning C-terminal segment of PLN [53] (see Fig. 10.2 for sequence similarities).

Because the contacts between rSLN and SERCA1a observed in the E1-Mg structures were similar to PLN–SERCA1a interactions inferred previously from cross-linking experiments [60–64], Toyoshima et al. and Winther et al. postulated

that the E1-Mg state is similar to the state that binds PLN [53, 54]. However, notable structural differences of their respective transmembrane domains indicate that PLN stabilizes a distinct conformation of SERCA1a. The Ca^{2+} binding sites in the E1-Mg structures are partially formed and have a distinctly E1-like appearance. On the other hand, in the metal-free E2 state that binds PLN, the SERCA transmembrane structure is closest to E2 state more than E1 state, leading to the collapse of the Ca^{2+} binding sites [59], suggesting that PLN and rSLN are interacting with different ATPase conformers.

Toyoshima et al. and Winther et al. made hypothesis concerning the binding or not of rSLN to different SERCA1a conformers during the catalytic cycle [53, 54]. Toyoshima et al. proposed that the E1.Mg^{2+} state is the preferred state for binding of rSLN as suggested previously for PLN [65, 46, 60, 64]. These authors suggested that rSLN cannot interact with the Ca_2.E1 and E2 states because, in these states, the position of the helices M2, M4, M6, and M9 leads to a very narrow and a very wide groove, respectively, that will prevent rSLN to bind firmly. Instead, Winther et al. suggested that the E2 state of SERCA1a is compatible with a SERCA1a–rSLN complex as the E2 structure offers a wider binding groove to rSLN [54]. In contrast, in the occluded Ca_2.E1P conformation, the position of the M1, M2, M3, and M4 helices leads to a narrowing of rSLN-binding site thus implicating rSLN dislodgement or a positional rearrangement. Recent cross-linking experiments suggest that rSLN remains in contact with the pump throughout the enzymatic cycle and, are thus in favor of a positional rearrangement of rSLN in interaction with SERCA1a [53]. Bidwell et al. demonstrate that a PLN–SERCA1a interaction remains even in presence of millimolar concentration of calcium or in presence of thapsigargin which may trigger the ATPase in a Ca_2.E1 or E2-like conformation, respectively [66].

8 Focus on Some Particular Features of Sarcolipin

8.1 Phosphorylation

Sequence analysis and site-directed mutagenesis experiments of Ser4 and Thr5 suggested that human, rat, and mouse SLN could be phosphorylated on Thr5 whereas rabbit, cow, and pig could be phosphorylated on Ser4 or Thr5 [33]. In this work, the effect of SLN overexpression and its ability to get phosphorylated were investigated in two different models. Using overexpression of the rabbit SERCA1a isoform in HEK-293 cells, in presence of wild-type (WT), S4A or T5A rabbit SLN, the authors demonstrated that both Ser4 and Thr5 are involved in the ATPase inhibition, Thr5 having probably a more preponderant role than Ser4. It is also shown that phosphorylation could be achieved by the Serine/Threonine-protein Kinase 16 (STK16, [67–70]). The overexpression of mouse SLN in mouse cardiac myocytes obtained from PLN null transgenic mice results in an inhibition of the cardiac function. Treatment with isoproterenol, a β-adrenoreceptor agonist and an activator of the cardiac muscle, resulted in complete restoration of the calcium dynamics in SLN

overexpressing tissues whereas no effect was found in absence of SLN. Therefore, a mechanism for which isoproterenol would act through cAMP signaling to regulate SLN interaction with SERCA isoforms is proposed. Bhupathy et al. demonstrated that a T5A point mutation exerts an inhibitory effect on rat myocyte contractility and calcium transients similar to that of WT SLN, whereas a phosphorylation mimetic mutation, T5E, abolishes the inhibition [32]. The WT and mutated SLN co-localized with SERCA2a in the rat ventricular myocytes sarcoplasmic reticulum. Interestingly, the overexpression of SLN has no effect on SERCA2a and PLN expression levels suggesting that the functional changes observed were really due to SLN. Similar results were obtained previously with PLN null transgenic mice [33], suggesting that SLN may act against SERCA2a independently of PLN (see below). Bhupathy et al. also proposed that SLN phosphorylation depends on the calcium/calmoduline-dependent protein Kinase II (CaMKII) rather on the STK16. The role of STK16 remains unclear whereas the role of CaMKII in heart is better known, especially CaMKII phosphorylates PLN at Thr17 during β-adrenergic-mediated stimulation and could be important for heart function [71–74]. However, no study investigates the possible role of Ser4.

Both Ser4 and Thr5 of SLN are close to SERCA1a Trp932 in the two recent structures of the SLN–SERCA1a complex [53, 54] and, molecular modeling of the phosphorylation of these two residues (Fig. 10.5) shows that in both cases, phosphorylation may induce steric clashes with Trp932 leading most probably to SLN and/or SERCA1a conformational changes. As a consequence, these conformational changes could induce dissociation of the complex as suggested by Toyoshima et al. [53].

Among 67 unique SLN sequences, most of them include a Ser and a Thr residue at positions 4 and 5, respectively, except for the rhinoceros which contains two successive threonines [31]. All the primates (9 species), including human, contain only Thr5, Ser4 being replaced by an asparagine (S4N). Note that Trp932 of SERCA isoforms 1a and 2a are fully conserved among mammals suggesting that some local rearrangement of the ATPase and/or the SLN N-terminus could take place when either Ser4 or Thr5 are substituted. Interestingly, most of the sequences from fishes (7 species among 8) contain only a serine at position 4, the threonine being replaced by an alanine (T5A) or a valine (T5V). Assuming that the regulatory mechanism of SERCA isoforms (and of muscle contraction) is conserved among species, i.e. dissociation of SLN from SERCA1a induced by phosphorylation, Ser4 will be a candidate for phosphorylation in fishes. Indeed, kinases like CaMKII are poorly specific [75] and thus, both Ser4 and Thr5 can be phosphorylation targets.

8.2 The RSYQY Luminal Tail

The C-terminus amino acid sequence of SLN, Arg^{27}-Ser-Tyr-Gln-Tyr (RSYQY tail), appears critical for its proper localization at the endoplasmic reticulum membrane, as it acts as an ER retention signal. Progressive amino acid deletion revealed that removal of the Arg27-Tyr31 sequence results in a misrouting of SLN. Interestingly, when the deleted form of SLN is co-expressed with SERCA2a,

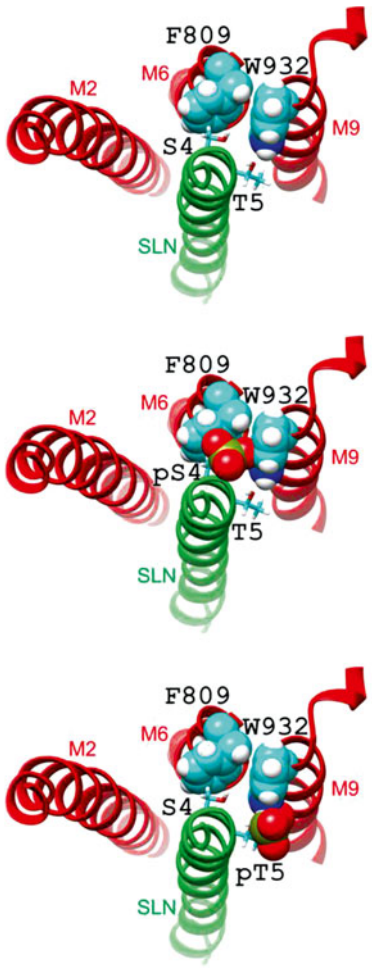

Fig. 10.5 Phosphorylation of rSLN Ser4 and Thr5. View from the cytosol of rSLN surrounded by the transmembrane helices M2, M6, and M9 of SERCA1a (PDB: 4H1W, [54]). *Top*: native rSLN; *middle*: model with rSLN Ser4 phosphorylated (*pS4*); *bottom*: model with rSLN Thr5 phosphorylated (*pT5*). Sarcolipin is depicted as a *green ribbon*. SERCA1a transmembrane helices M2, M6, and M9 are depicted as *red ribbons*. rSLN Ser4 and Thr5 side-chains are depicted as *sticks*. SERCA1a Phe809 and Trp932 side-chains are depicted as Van der Waal's spheres. Phosphorylated side-chains were modeled using UCSF Chimera software [103] and are depicted as Van der Waal's spheres. Carbon atoms are in cyan, oxygen in *red*, nitrogen in *blue*, phosphorus in bronze, and hydrogen in *white*

misrouting is abolished and this shortened form is stably expressed and properly co-localized with SERCA2a at the ER. It suggests that in presence of sufficient amount of a SERCA isoform, SLN can be addressed to the ER independently of its tail. However, it has been reported that in absence of SERCA, SLN may accumulate in the ER via interactions of its luminal tail with another partner [76].

A key role of this C-terminal tail for catalysis was pointed out early by MacLennan et al. [3] who showed that a C-terminally FLAG tagged version of SLN does not affect SERCA1a activities as WT or N-terminally tagged (NF) SLN isoforms. As a matter of fact, human, rat or rabbit SLN (hSLN, rat SLN, and NF-SLN respectively) induce a moderate decrease of $Ca_{1/2}$ (shifted from 0.35 μM in absence of SLN to 0.5 μM when SLN is co-expressed with SERCA1a in HEK-293 cells) and a significant increase of the Ca^{2+} uptake activity up to about 140 %. On the

other hand, co-expression of a C-terminally FLAG tagged rabbit SLN (SLN-FC) and SERCA1a resulted in a significant decrease of both $Ca_{1/2}$ (shifted from 0.35 μM to 1.1 μM) and V_{max} (only 62 % of the SERCA1a alone). To investigate the role of the tail in the regulation of SERCA1a, alanine mutants of the tail were co-reconstituted with native SERCA1a within proteoliposomes (SERCA1a:SLN:lipids 1:4.5:120 m:m:m, i.e. molar ratio close to those of native SR, [49, 50]). This study showed that, compared to the WT SLN, all the alanine mutants induced a lower inhibition of the SERCA1a, i.e. a moderate decrease of the affinity for calcium and a slight decrease of the V_{max}, except the Y31A mutant which induced an increase of the V_{max} despite a poor effect on the $Ca_{1/2}$ [50]. Note that these results are not in agreement with those previously published by MacLennan et al. [3]. Later, this group demonstrated that modifications of the tail sequence could trigger a misrouting of SLN as described above [76] suggesting that in HEK-293 cells, improper trafficking of mutated SLN was not taken into account in previous experiments. As a consequence, the co-reconstitution model seems to be a better model to investigate the effect of a complete amino acid deletion of the tail. Co-reconstitution of a ΔR27SLN with SERCA1a led to a smaller inhibition of the SERCA1a than for entire SLN ($Ca_{1/2}$ and V_{max} are closer to the SERCA1a alone values) [50]. However, in that model, the SERCA1a is from native rabbit SR membrane which already contains endogenous rabbit SLN. As mentioned above, SLN remains associated with the SERCA1a even after deoxycholate extraction or solubilization with mild detergent and subsequent purification [31]. Therefore, results from Gorski et al. were probably obtained in the presence of both endogenous WT SLN and recombinant—WT or mutated—SLN. However, considering the fact that a significant molar excess of SLN was used, those results suggest that SLN luminal tail is essential for the inhibition of the SERCA1a by SLN. The high degree of amino acid conservation of the Arg^{27}-Tyr-Gln residues also suggests a critical functional role of this sequence of SLN, a role that has survived evolutionary divergence [76, 31] (Fig. 10.3b). While SLN inhibition properties may reside in its luminal tail, most of the inhibition properties of PLN depend on its transmembrane region. As a matter of fact, the amino acid C-terminus sequences of SLN and PLN are rather different: Arg^{27}-Ser-Tyr-Gln-Tyr (RSYQY tail) for SLN and Met^{50}-Leu-Leu (MLL tail) for PLN in mammals. Furthermore, myoregulin is deprived of such a tail (Fig. 10.2), suggesting a mechanism of inhibition proper to each regulatory peptide. Recently, a very different amino acid sequence of the luminal tail was reported [77] for a zebrafish isoform of PLN (zfPLN) that comprises additional residues, Leu^{50}-Leu-Ile-Ser-Phe-His-Gly-Met (^{50}LLISPHGM). This luminal tail has different functional properties than those of SLN and other PLN isoforms and can only regulate SERCA1a in the context of the full primary sequence of zfPLN. Deletion of this tail resulted in a loss of inhibition by zfPLN and, a zfPLN–SLN_{tail} chimera restored the inhibition. A chimera composed of the human PLN and the luminal tail of zfPLN shares the same functional properties as human PLN suggesting that this tail is efficient only in a zebrafish context [77]. C-terminal residues are poorly defined in the two published crystal structures of the SLN–SERCA1a complexes due to missing electron density which probably reflects a high flexibility of this region [53, 54].

Thus, the hypothesis concerning the interaction between the luminal tail of SLN and the SERCA1a derived from experimental data [46, 50] could not be confirmed from these structures. However, solid state NMR studies showed that the peptide encompassing the five C-terminal residues (R^{27}SYQY) interacts with SERCA1a. Moreover, this peptide inhibits the ATPase activity, yet it has no effect on the $Ca_{1/2}$. Using various peptides differing by their length and amino acid composition, the authors proposed that the positively charged residue Arg27 may be important in stabilizing the interaction of the luminal tail with the SERCA1a, possibly through salt bridge formation, and that Tyr29 and Tyr31 could participate in π–π or π–cation interactions with residues from the luminal face of SERCA1a [43]. These interactions could not be confirmed by the crystal structures of the SLN–SERCA1a complexes due to the poorly defined structure of the C-terminal residues of SLN and of the luminal loop between M1 and M2.

8.3 S-Palmitoylation and S-Oleoylation of Cysteine 9

Recently, our group showed that native rabbit SLN is modified by a fatty acid anchor on its unique cysteine residue (Cys9) with a palmitic acid or, surprisingly, an oleic acid in a ratio of 60 % and 40 %, respectively [31]. Treatment with hydroxylamine removes the fatty acids from a majority of the SLN pool and apparently without any modification on the SERCA1a. Mass spectrometry analysis of SEC-purified samples after several hours of incubation confirmed that SLN is satisfactorily deacylated and that it remains associated with the SERCA1a even after solubilization by mild detergent like *n*-dodecyl-β-D-maltopyranoside (DDM) or octaethylene glycol monododecyl ether ($C_{12}E_8$) and successive purification of the complex by size exclusion chromatography [31]. This treatment does not modify the affinity of SERCA1a for Ca^{2+} but it results in an increase of the Ca^{2+}-dependent ATPase activity of native SR membranes indicating that the S-acylation is required for full inhibitory effect of rabbit SLN on rabbit SERCA1a (Fig. 10.6). Deacylation does not affect the stability of the Ca^{2+}ATPase over time, neither in a native membranous context nor after solubilization by mild detergent (*unpublished results*).

Sarcolipin is most probably acylated in the crystals [53, 54] as we found SLN acylated when it was purified in conditions very similar to the crystallization procedure [31]. Although no electron density exists to describe the position of the acyl chain (probably a consequence of a local disorder in the crystals), we propose a model of SLN palmitoylated on Cys9 in complex with SERCA1a and embedded in a POPC bilayer (Fig. 10.7). The acyl chain was grafted on the SLN Cys9 within the crystal structure of the complex [54]. As shown in Fig. 10.7, the acyl chain is inserted in the upper leaflet of the membrane and faces the lipids as Cys9 is located on the opposite side of the helix interaction side. It suggests that the acyl chain is probably not directly in contact with the Ca^{2+}-ATPase.

Alignment of 67 SLN amino acid sequences from different species shows that 19 of them contain a cysteine and the remaining sequences a phenylalanine at position 9. As an example, we demonstrated that pig SLN, obtained from *extensor digitorum*

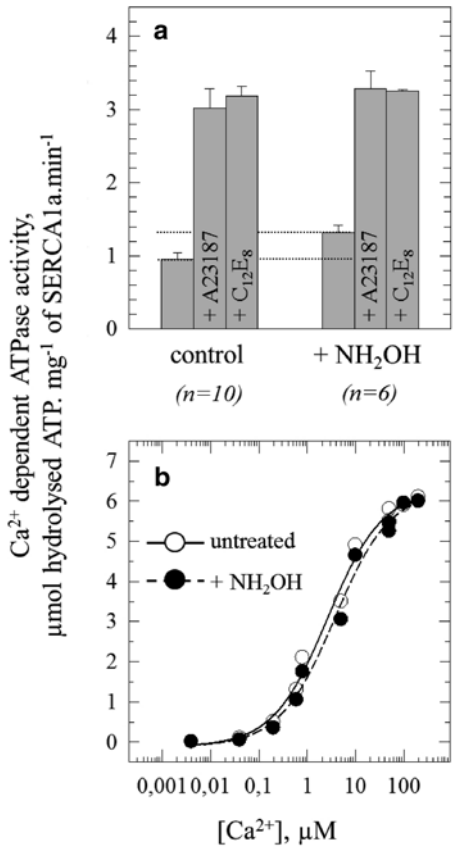

Fig. 10.6 Hydroxylamine treatment of SR membranes results in an increase of calcium ATPase activity but has a moderate effect on the apparent affinity for calcium. (**a**) Effect of hydroxylamine on ATPase activity. Rabbit SR membranes were initially suspended at 4 mg mL^{-1} in the assay buffer and stored on ice. When employed, an equal volume of a freshly prepared 2 M hydroxylamine solution (NH_2OH, pH adjusted at 7.5 with saturated Tris) was added prior to incubation at 20 °C for 1 h. As a control, an equal volume of buffer was added before incubation at 20 °C for 1 h. ATPase activity was estimated by an enzyme coupled assay as described previously [57] at pH 7.5 in presence of 50 µM free calcium (see [31] for further details). (**b**) Ca^{2+} dependency of the ATPase activity. ATPase activity was again measured by a coupled enzyme assay as described previously. The medium was first supplemented with 50 µM Ca^{2+} and subsequently with final Ca^{2+} concentrations of 100 or 200 µM, and then, various concentrations of EGTA were added sequentially, to explore the effect of lower free Ca^{2+} concentrations ($[Ca^{2+}]_{free}$ was estimated according to [104]). The medium also contained 0.1 mg/mL SR vesicles which have been formerly treated with 1 M hydroxylamine for 3 h at 20 °C (*black symbols and dashed line*) or not (3 h at 20 °C in absence of hydroxylamine; *empty symbols* and *continuous line*). Final concentration of hydroxylamine in the cuvette was 5 mM and has no effect on the enzyme coupled assay. These experiments have been done twice, each data point being the mean, and these data were fitted to Hill equations. *Error bars* were not indicated as they were smaller than the size of the symbols. The estimated $Ca_{1/2}$ for untreated and NH_2OH-treated SR are 2.3±0.3 µM (pCa=5.64) and 3.2±0.5 µM (pCa=5.49), respectively. Note that our values are higher than those indicated by MacLennan et al. who did the measurements at pH 7 [46], in conditions where the E2 to E1 equilibrium is pulled toward E2 resulting in slightly lower $Ca_{1/2}$ values

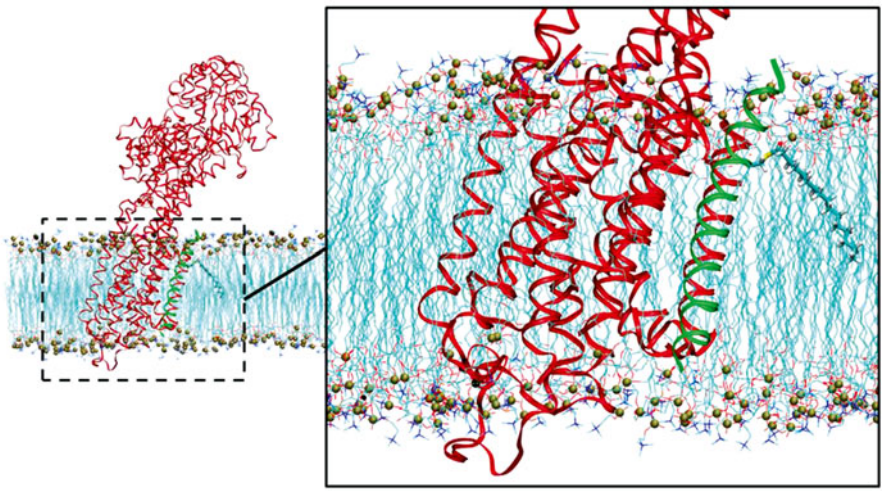

Fig. 10.7 Molecular modeling of Cys9-palmitoylated sarcolipin in interaction with SERCA1a embedded in a POPC bilayer. Molecular modeling of the palmitoylated SLN was made using UCSF Chimera software [103] and the SERCA1a/rSLN complex structure (PDB: 4H1W, [54]) as template. The complex was embedded in a POPC bilayer using the InflateGRO method [105] and data from the OPM database [106]. SERCA1a was tilted by 23° with respect to the membrane normal. Several energy minimization steps were performed using GROMACS [107] with protein atoms harmonically restrained using a force constant of 10,000 kcal mol^{-1} nm^{-2}. Snapshot representations are made using VMD software [108]. rSLN and SERCA1a are depicted as a *green* and a *red ribbon*, respectively. The palmitoyl anchor is represented in licorice and the POPC lipids are in sticks without the hydrogen atoms for the sake of clarity. Phosphorus atoms of POPC are represented as Van der Waal's spheres. Carbon atoms are in cyan, oxygen in *red*, nitrogen in *blue*, phosphorus in bronze, sulfur in *yellow*, and hydrogen in *white*

longus (EDL), is also fully palmitoylated/oleoylated and has the same properties as the rabbit SLN after deacylation. Based on a cladogram, we finally postulated that the phenylalanine mutation to cysteine in some species is the result of an evolutionary convergence. We proposed that, besides phosphorylation, S-acylation/deacylation may also regulate SLN activity [31]. Interestingly, acylation is also a feature that distinguishes sarcolipin from phospholamban: none of the three cysteines of PLN located within the membrane domain is acylated [78].

9 Does Sarcolipin Associate with Itself and with Phospholamban?

9.1 Does Sarcolipin Form Homo-Oligomers?

Considering the high degree of similarities between SLN and PLN transmembrane domain, the homo-oligomerization of SLN has been investigated because PLN forms stable pentamers [79, 80]. Indeed, the high-resolution structure of these

PLN pentamers was solved by NMR in the presence of DPC and reconstituted in a DOPC/DOPE bilayer [81, 82]. It has been proposed that this pentameric state should correspond to an inactive form of the PLN in equilibrium with a monomeric active form, the latter being able to interact with SERCA1a for inhibition. However, this hypothesis is challenged by the recent high-resolution crystal structure of a SERCA1a–PLN complex which shows that a dimeric and even a pentameric form of PLN could also interact with SERCA1a [59]. As a matter of fact, the residues involved in the pentamerization motif are localized at the opposite side of the helix than those implicated in the interaction with SERCA1a. It has been demonstrated that PLN homo-oligomerize via a Leucine zipper motif (Leu-x2-Ile-x3-Leu-x2-Ile-x3-Leu, [80–82]). No such motif can be found in SLN amino acid sequences suggesting that SLN, if able to interact with itself, homo-oligomerize via a different motif.

The oligomeric state of SLN was investigated by several groups [83–86, 43]. The study of the oligomerization of hSLN was performed in the presence of nonionic detergents and by centrifugation analysis and cross-linking experiments [86]. In these experiments, the authors show that both SLN and PLN form oligomers but that these oligomers greatly differ. Sarcolipin does not form SDS-resistant oligomers at concentration close to those used for PLN as shown by SDS-PAGE analysis. On contrary to PLN oligomers which are formed at low concentration reaching a pentameric equilibrium state, SLN oligomers appear only at much higher concentrations and seem to never reach a stable oligomeric state as the size of the oligomer increases linearly as a function of SLN concentration. In addition, SLN oligomers were observed by cross-linking in POPC liposomes but only in the presence of a very large excess of cross-linker. Analysis of SLN oligomer formation after reconstitution in DOPC bilayers by solid-state NMR reveals that SLN remains monomeric at millimolar concentration [43].

It has also been suggested that oligomerization of SLN could result in a pore formation as proposed for PLN [83–85]. To demonstrate the formation of pores, SLN was incorporated into a supported lipid bilayer anchored to a mercury electrode through a hydrophilic tetraethyleneoxy chain. As a matter of fact, lipid bilayers tethered to a metal surface via a hydrophilic "spacer," often called tethered bilayer lipid membranes (tBLMs), may provide a friendly environment to channel-forming peptides and proteins, thus maintaining their functionally active state and allowing an investigation of their putative function. Adding inorganic anions as chloride, sulfate, phosphate, or oxalate in the presence of SLN leads to an increase of the tBLM conductivity whereas the same experiment using inorganic cations does not show a modification of the membrane conductivity. This could suggest that sarcolipin aggregates into an anion-conducting-like pore. But, such a permeabilization cannot occur at physiological pH [84]. The authors suggested that sarcolipin pore activity should participate in the dissipation of the local increase of the luminal transmembrane potential caused by proton counter transport and the translocation in the lumen of the phosphate ions resulting from ATP hydrolysis [83]. Even if the SLN channel permeabilizing effect observed for phosphate ions is modest compared to the ATPase activity, such a translocation of phosphate should improve the

accumulation of calcium in the lumen and limit retro-inhibition of the SERCA1a, resulting in an increase of the turnover at millimolar concentration of calcium as suggested initially by MacLennan et al. [3]. Nevertheless, it has to be considered that SLN oligomerization is observed here in supported DOPC monolayers, an in vitro model which is very different from a natural bilayer. Because SLN is a transmembrane peptide, its insertion in a lipid monolayer instead of a bilayer could artificially favor its oligomerization. Smith et al. have demonstrated that co-reconstitution of SLN with native SR membrane does not permeabilize the membrane neither to calcium nor to proton [20]. Moreover, SERCA1a acts as a Ca^{2+}/H^{+}-ATPase (Fig. 10.1), and since the bilayer is impermeable to protons, addition of FCCP, a protonophore, to the vesicles resulted in an increase of the accumulation of calcium [87]. Smith et al. showed that even in the presence of a SLN:SERCA1a 5:1 mol:mol ratio, the greatest accumulation of calcium observed in the presence of FCCP, remains the same as in the control experiment done in the absence of SLN, demonstrating that SLN does not form oligomers leaky to protons [20]. The divergent results found in the literature suggest that the putative oligomerization of SLN has to be carefully investigated in a natural environment in order to validate the relevancy of such mechanism in the context of the regulation of SERCA isoforms and of the SR calcium homeostasis.

9.2 Do SLN and PLN Interact?

Similarly to the ongoing discussion of homo-oligomerization of SLN, the potential interaction of SLN with PLN is also currently under debate. Since SLN and PLN are co-expressed in the *atria* and in several smooth or fast-twitch muscle [4, 12], possible ternary interactions of those two peptides and the rabbit SERCA1a or rabbit SERCA2a isoforms were investigated [45]. Co-overexpression of SLN, PLN, and SERCA isoforms in HEK-293 cells led to a super-inhibition of the calcium uptake in microsomes: calcium affinity decreased by one order of magnitude (at pH 7, $Ca_{1/2SERCA1a\ alone}$ = 0.35 μM, $Ca_{1/2SERCA1a+PLN}$ = 0.79 μM, $Ca_{1/2SERCA1a+SLN}$ = 0.58 μM, $Ca_{1/2SERCA1a+PLN+SLN}$ = 3.0 μM) and the V_{max}, which was not affected by the expression of only one regulatory peptide, decreased by 20 % for SERCA1a and 50 % for SERCA2a. Using molecular modeling, the authors firstly suggested that a SERCA1a/PLN/SLN ternary complex could be formed (E2-like structure used as SERCA1a model, [58]) with both SLN and PLN in close contact with SERCA1a [46]). However, the same authors recently rejected this hypothesis arguing that the binding groove of SLN within the SERCA1a–SLN complex is too narrow to accommodate an additional transmembrane helix like that of PLN [53]. The high-resolution structure of SERCA1a–SLN complex was obtained using native sarcoplasmic reticulum membrane as protein sources. The structure of the groove is conserved in the high-resolution structure of SERCA1a obtained using a recombinant SLN-free source and the same conditions of crystallization [88–90, 53]. Thus, this suggests that the groove size is governed by the state of the ATPase and not induced by the presence of SLN (or PLN).

It has been proposed that SLN could destabilize PLN pentamers and that this destabilization could result in an increase in PLN monomers and in a super-inhibition of SERCAs. As a matter of fact, site-directed mutagenesis study of phospholamban showed that the equilibrium between the pentameric form ("inactive" form) and the monomeric form ("active" inhibitory form) influences the ATPase activity [91]. Mutations of key residues of the leucine zipper motif induced depolymerization of PLN and an increase in its inhibitory effect on SERCA2a. To date, this super-inhibitory activity is not clearly demonstrated in vivo. In addition, in the co-overexpression experiments, the stoichiometry of SLN, PLN or SERCA isoforms which is not indicated could be a source of misinterpretation. It is not demonstrated that the level of expression of the regulatory peptides is sufficient to exert a maximum inhibitory effect on the overexpressed ATPase. As pointed out above, the effect of SLN on the $Ca_{1/2}$ or the V_{max} depends on the system used to characterize the inhibition. Moreover, the expression levels of SLN and PLN in vivo are still a matter of debate [92] so caution should be taken not to misinterpret the in vitro data in a physiological context.

10 Conclusions

The role of sarcolipin in SERCAs regulation is complex and still subject to debate. Sarcolipin is regulated itself at several levels from the gene to the protein. The presence in myocytes of particular transcription factors (myocyte enhancer factor) is probably responsible of its muscle-specific expression. Furthermore, the presence of different polyadenylation signals among species could also result in differences at the final translation level. Several data are now available on the expression level of SLN from different tissues and from different species. It has been clearly demonstrated that SLN is expressed in several tissues, even in the presence of other regulatory peptides like phospholamban. Sarcolipin expression is not restricted to fast-twitch muscle as initially proposed. The level of expression in one particular tissue from one species to another could also greatly vary, for example, the amount of SLN in the mouse skeletal muscle is about one thousand time lower than in rabbit skeletal muscle [92]. All these data indicate that expression of SLN is fine-tuned at many levels, even before its interaction with Ca^{2+}-ATPases or putative other partners. In addition, interaction of SLN with Ca^{2+}-ATPases is regulated by post-translational modifications. Phosphorylation of its N-terminus, via the β-adrenergic calcium regulation pathway, could trigger its dissociation from the Ca^{2+}-ATPases. Recently, it has been demonstrated that sarcolipin is also S-palmitoylated and S-oleoylated. The exact role of these latter modifications is still unknown but it has been reported that acylation could affect membrane protein localization, stabilization within the membrane, and interaction with other proteins [93]. To date, SLN is the only SERCAs regulatory peptide which is acylated. Interestingly, it is now clear that SLN and PLN do not share the same regulatory mechanism. The recent high-resolution structures of the SERCA1a–SLN complex [53, 54] illustrate and give

new insights into how SLN inhibition arises from the stabilization of a Ca^{2+}-free E1 intermediate state. However, these structures and the comparison with the recent structure of SERCA1a–PLN complex [59] raise the following question: what are the structural and dynamic features of both partners (peptides and SERCAs) that are important for the regulation of SERCAs knowing that SLN and PLN are sometimes expressed in the same cells, at the same time, and in similar amounts [12]? Moreover, although rabbit SERCA1a and human SERCA2a share a high degree of identity (about 85 %), it is worth to mention the presence of a small patch of different amino acids in the N-domain. Many residues from this patch belong to the interaction site of the PLN N-terminus with the SERCAs N-domain, so it could explain part of the functional differences between PLN and SLN as SLN has not such an N-terminal extension [94–96]. Furthermore, the life time of the SLN–SERCAs complex during catalysis remains unclear. The hypothesis that SLN could interact only with a particular catalytic state and the hypothesis that SLN could remain bound to the SERCAs during the whole cycle are both considered in the literature. For example, based on a docking analysis, Winther et al. suggest that sarcolipin does not bind to the Ca_2.E1P state as the groove is too narrow [54]. However, we observed that the complex remains formed even in presence of saturating concentration of calcium and of AMPCP which may trigger the ATPase in a Ca_2.E1P-like conformation (*unpublished results*).

Numerous studies have recently documented the role of SLN in muscle-based thermogenesis. It has been shown that expression of SLN increases the uncoupling of the ATPase and, consequently the rate of heat production [24, 25]. Furthermore, knock-out mice ($SLN^{-/-}$) or SLN overexpressing mice (SLN^{OE}) were recently extensively used to determine the possible role of SLN in several metabolic pathways [28, 29, 97]. Knock-out mice have a lower body temperature so it suggests that SLN expression is probably critical for cold-induced muscle-based thermogenesis, probably via its interaction with SERCA1a [28, 29]. Additionally, SLN^{OE} mice displayed a higher oxygen consumption and fatty acid oxidation than wild-type mice suggesting a diet-induced thermogenesis [98]. An increase of SLN expression seems to improve skeletal muscle performance by reducing fatigue during a prolonged activity [97]. However, the use of $SLN^{-/-}$ or SLN^{OE} mice was recently debated due to the low level of SLN expression in wild-type mice skeletal muscles. It is unlikely that deleting SLN would have an assessable effect on thermogenesis by the calcium pumps [92]. As rodents possess brown adipose tissue physiologically essentially dedicated to heat production, they probably do not need another efficient muscle-based heat production pathway. Nevertheless, SLN might have a role in muscle-based thermogenesis in larger mammals, most of them being deprived from such brown adipose tissues [99].

Given the importance of SERCAs pump activity in regulating Ca^{2+} handling and the pathogenesis of skeletal muscle diseases, such as myopathy and muscular dystrophies, the recent discovery of several putative regulatory peptides opens interesting possibilities for the treatment of these diseases [7]. It suggests that expression of the different regulatory peptides could act with compensatory effects as MLN might be expressed in SLN- and PLN-deprived mice tissues [7]. However, at the present

time, myoregulin peptides were not detected in vivo [7, 8]: their expression level compared to SLN and PLN in different species and tissues has to be investigated. Interestingly, the sequence coding MLN was found in a mistakenly annotated noncoding mRNA specific from skeletal muscle. Consequently, several unidentified regulatory peptides could also be encoded in the many mRNA sequences currently annotated as noncoding sequences, and their discovery would open the way to a better knowledge of muscle physiology.

Acknowledgments This work was supported by the French Infrastructure for Integrated Structural Biology (FRISBI) and by grants from the Agence Nationale pour la Recherche and the Ile de France region (Domaine d'Intérêt Majeur Maladies Infectieuses, DIM MALINF).

References

1. Wawrzynow A, Theibert JL, Murphy C et al (1992) Sarcolipin, the "proteolipid" of skeletal muscle sarcoplasmic reticulum, is a unique, amphipathic, 31-residue peptide. Arch Biochem Biophys 298:620–623
2. MacLennan D, Yip C, Iles G et al (1972) Isolation of sarcoplasmic reticulum proteins. Cold Spring Harb Symp Quant Biol 37:469–477
3. Odermatt A, Becker S, Khanna VK et al (1998) Sarcolipin regulates the activity of SERCA1, the fast-twitch skeletal muscle sarcoplasmic reticulum Ca2+-ATPase. J Biol Chem 273:12360–12369
4. Odermatt A, Taschner PE, Scherer SW et al (1997) Characterization of the gene encoding human sarcolipin (SLN), a proteolipid associated with SERCA1: absence of structural mutations in five patients with Brody disease. Genomics 45:541–553
5. Moller JV, Juul B, le Maire M (1996) Structural organization, ion transport, and energy transduction of P-type ATPases. Biochim Biophys Acta 1286:1–51
6. Kirchberber MA, Tada M, Katz AM (1975) Phospholamban: a regulatory protein of the cardiac sarcoplasmic reticulum. Recent Adv Stud Cardiac Struct Metab 5:103–115
7. Anderson DM, Anderson KM, Chang CL et al (2015) A micropeptide encoded by a putative long noncoding RNA regulates muscle performance. Cell 160:595–606
8. Magny EG, Pueyo JI, Pearl FM et al (2013) Conserved regulation of cardiac calcium uptake by peptides encoded in small open reading frames. Science 341:1116–1120
9. Weintraub H, Davis R, Lockshon D et al (1990) MyoD binds cooperatively to two sites in a target enhancer sequence: occupancy of two sites is required for activation. Proc Natl Acad Sci U S A 87:5623–5627
10. Piette J, Bessereau JL, Huchet M et al (1990) Two adjacent MyoD1-binding sites regulate expression of the acetylcholine receptor alpha-subunit gene. Nature 345:353–355
11. Kozak M (1987) At least six nucleotides preceding the AUG initiator codon enhance translation in mammalian cells. J Mol Biol 196:947–950
12. Vangheluwe P, Schuermans M, Zador E et al (2005) Sarcolipin and phospholamban mRNA and protein expression in cardiac and skeletal muscle of different species. Biochem J 389:151–159
13. Babu GJ, Bhupathy P, Carnes CA et al (2007) Differential expression of sarcolipin protein during muscle development and cardiac pathophysiology. J Mol Cell Cardiol 43:215–222
14. Fajardo VA, Bombardier E, Vigna C et al (2013) Co-expression of SERCA isoforms, phospholamban and sarcolipin in human skeletal muscle fibers. PLoS One 8, e84304
15. Uemura N, Ohkusa T, Hamano K et al (2004) Down-regulation of sarcolipin mRNA expression in chronic atrial fibrillation. Eur J Clin Invest 34:723–730

16. Shanmugam M, Molina CE, Gao S et al (2011) Decreased sarcolipin protein expression and enhanced sarco(endo)plasmic reticulum Ca2+ uptake in human atrial fibrillation. Biochem Biophys Res Commun 410:97–101
17. Vittorini S, Storti S, Parri MS et al (2007) SERCA2a, phospholamban, sarcolipin, and ryanodine receptors gene expression in children with congenital heart defects. Mol Med 13:105–111
18. Guglielmi V, Vattemi G, Gualandi F et al (2013) SERCA1 protein expression in muscle of patients with Brody disease and Brody syndrome and in cultured human muscle fibers. Mol Genet Metab 110:162–169
19. Block BA (1994) Thermogenesis in muscle. Annu Rev Physiol 56:535–577
20. Smith WS, Broadbridge R, East JM et al (2002) Sarcolipin uncouples hydrolysis of ATP from accumulation of Ca2+ by the Ca2+-ATPase of skeletal-muscle sarcoplasmic reticulum. Biochem J 361:277–286
21. de Meis L (1998) Control of heat produced during ATP hydrolysis by the sarcoplasmic reticulum Ca(2+)-ATPase in the absence of a Ca2+ gradient. Biochem Biophys Res Commun 243:598–600
22. Mitidieri F, de Meis L (1999) Ca(2+) release and heat production by the endoplasmic reticulum Ca(2+)-ATPase of blood platelets. Effect of the platelet activating factor. J Biol Chem 274:28344–28350
23. de Meis L (2001) Role of the sarcoplasmic reticulum Ca2+-ATPase on heat production and thermogenesis. Biosci Rep 21:113–137
24. de Meis L (2001) Uncoupled ATPase activity and heat production by the sarcoplasmic reticulum Ca2+-ATPase. Regulation by ADP. J Biol Chem 276:25078–25087
25. Lee AG (2002) A calcium pump made visible. Curr Opin Struct Biol 12:547–554
26. Mall S, Broadbridge R, Harrison SL et al (2006) The presence of sarcolipin results in increased heat production by Ca(2+)-ATPase. J Biol Chem 281:36597–36602
27. Stammers AN, Susser SE, Hamm NC et al (2015) The regulation of sarco(endo)plasmic reticulum calcium-ATPases (SERCA). Can J Physiol Pharmacol 19:1–12
28. Bal NC, Maurya SK, Sopariwala DH et al (2012) Sarcolipin is a newly identified regulator of muscle-based thermogenesis in mammals. Nat Med 18:1575–1579
29. Bombardier E, Smith IC, Vigna C et al (2013) Ablation of sarcolipin decreases the energy requirements for Ca2+ transport by sarco(endo)plasmic reticulum Ca2+-ATPases in resting skeletal muscle. FEBS Lett 587:1687–1692
30. Gillard EF, Otsu K, Fujii J et al (1991) A substitution of cysteine for arginine 614 in the ryanodine receptor is potentially causative of human malignant hyperthermia. Genomics 11:751–755
31. Montigny C, Decottignies P, Le Marechal P et al (2014) S-palmitoylation and s-oleoylation of rabbit and pig sarcolipin. J Biol Chem 289:33850–33861
32. Bhupathy P, Babu GJ, Ito M et al (2009) Threonine-5 at the N-terminus can modulate sarcolipin function in cardiac myocytes. J Mol Cell Cardiol 47:723–729
33. Gramolini AO, Trivieri MG, Oudit GY et al (2006) Cardiac-specific overexpression of sarcolipin in phospholamban null mice impairs myocyte function that is restored by phosphorylation. Proc Natl Acad Sci U S A 103:2446–2451
34. Montaville P, Jamin N (2010) Determination of membrane protein structures using solution and solid-state NMR. Methods Mol Biol 654:261–282
35. Warschawski DE, Arnold AA, Beaugrand M et al (2011) Choosing membrane mimetics for NMR structural studies of transmembrane proteins. Biochim Biophys Acta 1808: 1957–1974
36. Mascioni A, Karim C, Barany G et al (2002) Structure and orientation of sarcolipin in lipid environments. Biochemistry 41:475–482
37. Buck B, Zamoon J, Kirby TL et al (2003) Overexpression, purification, and characterization of recombinant Ca-ATPase regulators for high-resolution solution and solid-state NMR studies. Protein Expr Purif 30:253–261

38. Buffy JJ, Buck-Koehntop BA, Porcelli F et al (2006) Defining the intramembrane binding mechanism of sarcolipin to calcium ATPase using solution NMR spectroscopy. J Mol Biol 358:420–429
39. Buffy JJ, Traaseth NJ, Mascioni A et al (2006) Two-dimensional solid-state NMR reveals two topologies of sarcolipin in oriented lipid bilayers. Biochemistry 45:10939–10946
40. Shi L, Cembran A, Gao J et al (2009) Tilt and azimuthal angles of a transmembrane peptide: a comparison between molecular dynamics calculations and solid-state NMR data of sarcolipin in lipid membranes. Biophys J 96:3648–3662
41. De Simone A, Mote KR, Veglia G (2014) Structural dynamics and conformational equilibria of SERCA regulatory proteins in membranes by solid-state NMR restrained simulations. Biophys J 106:2566–2576
42. Traaseth NJ, Ha KN, Verardi R et al (2008) Structural and dynamic basis of phospholamban and sarcolipin inhibition of Ca(2+)-ATPase. Biochemistry 47:3–13
43. Hughes E, Clayton JC, Kitmitto A et al (2007) Solid-state NMR and functional measurements indicate that the conserved tyrosine residues of sarcolipin are involved directly in the inhibition of SERCA1. J Biol Chem 282:26603–26613
44. Shaw G, Morse S, Ararat M et al (2002) Preferential transformation of human neuronal cells by human adenoviruses and the origin of HEK 293 cells. FASEB J 16:869–871
45. Asahi M, Kurzydlowski K, Tada M et al (2002) Sarcolipin inhibits polymerization of phospholamban to induce superinhibition of sarco(endo)plasmic reticulum Ca2+-ATPases (SERCAs). J Biol Chem 277:26725–26728
46. Asahi M, Sugita Y, Kurzydlowski K et al (2003) Sarcolipin regulates sarco(endo)plasmic reticulum Ca2+-ATPase (SERCA) by binding to transmembrane helices alone or in association with phospholamban. Proc Natl Acad Sci U S A 100:5040–5045
47. MacLennan DH, Asahi M, Tupling AR (2003) The regulation of SERCA-type pumps by phospholamban and sarcolipin. Ann N Y Acad Sci 986:472–480
48. Hughes E, Middleton DA (2003) Solid-state NMR reveals structural changes in phospholamban accompanying the functional regulation of Ca2+-ATPase. J Biol Chem 278:20835–20842
49. Douglas JL, Trieber CA, Afara M et al (2005) Rapid, high-yield expression and purification of Ca2+-ATPase regulatory proteins for high-resolution structural studies. Protein Expr Purif 40:118–125
50. Gorski PA, Glaves JP, Vangheluwe P et al (2013) Sarco(endo)plasmic reticulum calcium ATPase (SERCA) inhibition by sarcolipin is encoded in its luminal tail. J Biol Chem 288:8456–8467
51. Tupling AR, Asahi M, MacLennan DH (2002) Sarcolipin overexpression in rat slow twitch muscle inhibits sarcoplasmic reticulum Ca2+ uptake and impairs contractile function. J Biol Chem 277:44740–44746
52. Pardi A, Wagner G, Wuthrich K (1983) Protein conformation and proton nuclear-magnetic-resonance chemical shifts. Eur J Biochem 137:445–454
53. Toyoshima C, Iwasawa S, Ogawa H et al (2013) Crystal structures of the calcium pump and sarcolipin in the Mg2+-bound E1 state. Nature 495:260–264
54. Winther AM, Bublitz M, Karlsen JL et al (2013) The sarcolipin-bound calcium pump stabilizes calcium sites exposed to the cytoplasm. Nature 495:265–269
55. Lund S, Orlowski S, de Foresta B et al (1989) Detergent structure and associated lipid as determinants in the stabilization of solubilized Ca2+-ATPase from sarcoplasmic reticulum. J Biol Chem 264:4907–4915
56. Montigny C, Arnou B, Champeil P (2010) Glycyl betaine is effective in slowing down the irreversible denaturation of a detergent-solubilized membrane protein, sarcoplasmic reticulum Ca2+-ATPase (SERCA1a). Biochem Biophys Res Commun 391:1067–1069
57. Montigny C, Arnou B, Marchal E et al (2008) Use of glycerol-containing media to study the intrinsic fluorescence properties of detergent-solubilized native or expressed SERCA1a. Biochemistry 47:12159–12174

58. Toyoshima C, Nomura H (2002) Structural changes in the calcium pump accompanying the dissociation of calcium. Nature 418:605–611
59. Akin BL, Hurley TD, Chen Z et al (2013) The structural basis for phospholamban inhibition of the calcium pump in sarcoplasmic reticulum. J Biol Chem 288:30181–30191
60. Chen Z, Akin BL, Stokes DL et al (2006) Cross-linking of C-terminal residues of phospholamban to the Ca2+ pump of cardiac sarcoplasmic reticulum to probe spatial and functional interactions within the transmembrane domain. J Biol Chem 28:14163–14172
61. Chen Z, Stokes DL, Jones LR (2005) Role of leucine 31 of phospholamban in structural and functional interactions with the Ca2+ pump of cardiac sarcoplasmic reticulum. J Biol Chem 280:10530–10539
62. Chen Z, Stokes DL, Rice WJ et al (2003) Spatial and dynamic interactions between phospholamban and the canine cardiac Ca2+ pump revealed with use of heterobifunctional cross-linking agents. J Biol Chem 278:48348–48356
63. Jones LR, Cornea RL, Chen Z (2002) Close proximity between residue 30 of phospholamban and cysteine 318 of the cardiac Ca2+ pump revealed by intermolecular thiol cross-linking. J Biol Chem 277:28319–28329
64. Toyoshima C, Asahi M, Sugita Y et al (2003) Modeling of the inhibitory interaction of phospholamban with the Ca2+ ATPase. Proc Natl Acad Sci U S A 100:467–472
65. Akin BL, Chen Z, Jones LR (2010) Superinhibitory phospholamban mutants compete with Ca2+ for binding to SERCA2a by stabilizing a unique nucleotide-dependent conformational state. J Biol Chem 285:28540–28552
66. Bidwell P, Blackwell DJ, Hou Z et al (2011) Phospholamban binds with differential affinity to calcium pump conformers. J Biol Chem 286:35044–35050
67. Berson AE, Young C, Morrison SL et al (1999) Identification and characterization of a myristylated and palmitylated serine/threonine protein kinase. Biochem Biophys Res Commun 259:533–538
68. Kurioka K, Nakagawa K, Denda K et al (1998) Molecular cloning and characterization of a novel protein serine/threonine kinase highly expressed in mouse embryo. Biochim Biophys Acta 1443:275–284
69. Ligos JM, Gerwin N, Fernandez P et al (1998) Cloning, expression analysis, and functional characterization of PKL12, a member of a new subfamily of ser/thr kinases. Biochem Biophys Res Commun 249:380–384
70. Stairs DB, Perry Gardner H, Ha SI et al (1998) Cloning and characterization of Krct, a member of a novel subfamily of serine/threonine kinases. Hum Mol Genet 7:2157–2166
71. MacLennan DH, Kranias EG (2003) Phospholamban: a crucial regulator of cardiac contractility. Nat Rev Mol Cell Biol 4:566–577
72. Simmerman HK, Jones LR (1998) Phospholamban: protein structure, mechanism of action, and role in cardiac function. Physiol Rev 78:921–947
73. Tada M, Kadoma M (1989) Regulation of the Ca2+ pump ATPase by cAMP-dependent phosphorylation of phospholamban. Bioessays 10:157–163
74. Zhao W, Uehara Y, Chu G et al (2004) Threonine-17 phosphorylation of phospholamban: a key determinant of frequency-dependent increase of cardiac contractility. J Mol Cell Cardiol 37:607–612
75. Ubersax JA, Ferrell JE Jr (2007) Mechanisms of specificity in protein phosphorylation. Nat Rev Mol Cell Biol 8:530–541
76. Gramolini AO, Kislinger T, Asahi M et al (2004) Sarcolipin retention in the endoplasmic reticulum depends on its C-terminal RSYQY sequence and its interaction with sarco(endo) plasmic Ca(2+)-ATPases. Proc Natl Acad Sci U S A 101:16807–16812
77. Gorski PA, Trieber CA, Ashrafi G et al (2015) Regulation of the sarcoplasmic reticulum calcium pump by divergent phospholamban isoforms in zebrafish. J Biol Chem 290: 6777–6788
78. Mayer EJ, McKenna E, Garsky VM et al (1996) Biochemical and biophysical comparison of native and chemically synthesized phospholamban and a monomeric phospholamban analog. J Biol Chem 271:1669–1677

79. Arkin IT, Adams PD, Brunger AT et al (1997) Structural perspectives of phospholamban, a helical transmembrane pentamer. Annu Rev Biophys Biomol Struct 26:157–179
80. Simmerman HK, Kobayashi YM, Autry JM et al (1996) A leucine zipper stabilizes the pentameric membrane domain of phospholamban and forms a coiled-coil pore structure. J Biol Chem 271:5941–5946
81. Traaseth NJ, Verardi R, Torgersen KD et al (2007) Spectroscopic validation of the pentameric structure of phospholamban. Proc Natl Acad Sci U S A 104:14676–14681
82. Verardi R, Shi L, Traaseth NJ et al (2011) Structural topology of phospholamban pentamer in lipid bilayers by a hybrid solution and solid-state NMR method. Proc Natl Acad Sci U S A 108(22):9101–9106
83. Becucci L, Foresti ML, Schwan A et al (2013) Can proton pumping by SERCA enhance the regulatory role of phospholamban and sarcolipin? Biochim Biophys Acta 1828:2682–2690
84. Becucci L, Guidelli R, Karim CB et al (2007) An electrochemical investigation of sarcolipin reconstituted into a mercury-supported lipid bilayer. Biophys J 93:2678–2687
85. Becucci L, Guidelli R, Karim CB et al (2009) The role of sarcolipin and ATP in the transport of phosphate ion into the sarcoplasmic reticulum. Biophys J 97:2693–2699
86. Hellstern S, Pegoraro S, Karim CB et al (2001) Sarcolipin, the shorter homologue of phospholamban, forms oligomeric structures in detergent micelles and in liposomes. J Biol Chem 27630845–30852
87. Levy D, Seigneuret M, Bluzat A et al (1990) Evidence for proton countertransport by the sarcoplasmic reticulum Ca2(+)-ATPase during calcium transport in reconstituted proteoliposomes with low ionic permeability. J Biol Chem 265:19524–19534
88. Clausen JD, Bublitz M, Arnou B et al (2014) SERCA mutant E309Q binds two Ca(2+) ions but adopts a catalytically incompetent conformation. EMBO J 32:3231–3243
89. Jidenko M, Nielsen RC, Sorensen TL et al (2005) Crystallization of a mammalian membrane protein overexpressed in Saccharomyces cerevisiae. Proc Natl Acad Sci U S A 102: 11687–11691
90. Marchand A, Winther AM, Holm PJ et al (2008) Crystal structure of D351A and P312A mutant forms of the mammalian sarcoplasmic reticulum Ca(2+) -ATPase reveals key events in phosphorylation and Ca(2+) release. J Biol Chem 283:14867–14882
91. Kimura Y, Kurzydlowski K, Tada M et al (1997) Phospholamban inhibitory function is activated by depolymerization. J Biol Chem 272:15061–15064
92. Butler J, Smyth N, Broadbridge R et al (2015) The effects of sarcolipin over-expression in mouse skeletal muscle on metabolic activity. Arch Biochem Biophys 569:26–31
93. Charollais J, Van Der Goot FG (2009) Palmitoylation of membrane proteins (Review). Mol Membr Biol 26:55–66
94. Toyofuku T, Kurzydlowski K, Tada M et al (1993) Identification of regions in the Ca(2+)-ATPase of sarcoplasmic reticulum that affect functional association with phospholamban. J Biol Chem 268:2809–2815
95. Toyofuku T, Kurzydlowski K, Tada M et al (1994) Amino acids Glu2 to Ile18 in the cytoplasmic domain of phospholamban are essential for functional association with the Ca(2+)-ATPase of sarcoplasmic reticulum. J Biol Chem 269:3088–3094
96. Toyofuku T, Kurzydlowski K, Tada M et al (1994) Amino acids Lys-Asp-Asp-Lys-Pro--Val402 in the Ca(2+)-ATPase of cardiac sarcoplasmic reticulum are critical for functional association with phospholamban. J Biol Chem 269:22929–22932
97. Sopariwala DH, Pant M, Shaikh SA et al (2015) Sarcolipin overexpression improves muscle energetics and reduces fatigue. J Appl Physiol 118:1050–1058
98. Maurya SK, Bal NC, Sopariwala DH et al (2015) Sarcolipin is a key determinant of basal metabolic rate and its overexpression enhances energy expenditure and resistance against diet induced obesity. J Biol Chem 24:840–849
99. Gamu D, Bombardier E, Smith IC et al (2014) Sarcolipin provides a novel muscle-based mechanism for adaptive thermogenesis. Exerc Sport Sci Rev 42:136–142
100. Galtier N, Gouy M, Gautier C (1996) SEAVIEW and PHYLO_WIN: two graphic tools for sequence alignment and molecular phylogeny. Comput Appl Biosci 12:543–548

101. Crooks GE, Hon G, Chandonia JM et al (2004) WebLogo: a sequence logo generator. Genome Res 14:1188–1190
102. Schneider TD, Stephens RM (1990) Sequence logos: a new way to display consensus sequences. Nucleic Acids Res 18:6097–6100
103. Pettersen EF, Goddard TD, Huang CC et al (2004) UCSF Chimera--a visualization system for exploratory research and analysis. J Comput Chem 25:1605–1612
104. Bers DM, Patton CW, Nuccitelli R (2010) A practical guide to the preparation of Ca(2+) buffers. Methods Cell Biol 99:1–26
105. Kandt C, Ash WL, Tieleman DP (2007) Setting up and running molecular dynamics simulations of membrane proteins. Methods 41:475–488
106. Lomize MA, Pogozheva ID, Joo H et al (2012) OPM database and PPM web server: resources for positioning of proteins in membranes. Nucleic Acids Res 40(Database issue):D370–376
107. Pronk S, Pall S, Schulz R et al (2013) GROMACS 4.5: a high-throughput and highly parallel open source molecular simulation toolkit. Bioinformatics 29:845–854
108. Humphrey W, Dalke A, Schulten K (1996) VMD: visual molecular dynamics. J Mol Graph 14(33-38):27–38